ASTRONOMY & ASTROPHYSICS
SUPPLEMENT SERIES

FEBRUARY I **1999**, PAGE 401

Astron. Astrophys. Suppl. Ser. **134**, 401–436 (1999)

VLA observations of a 4C equatorial sample. II.

N. Jackson[1], **J. Roland**[2], **M. Bremer**[2], **G. Rhee**[3], **and J. Webb**[4]

[1] University of Manchester, NRAL, Jodrell Bank, Macclesfield SK11 9DL, UK
[2] Institut d'Astrophysique, 98 bis Blvd. Arago, 75014 Paris, France
[3] Physics Department, Box 4002, UNLV, Las Vegas, NV89195, U.S.A.
[4] School of Physics, University of New South Wales, Sydney, Australia

Received January 16; accepted July 3, 1998

Abstract. We present VLA observations at 4.9 GHz of 144 steep-spectrum 4C sources whose declinations are between $-4°$ and $4°$ and whose angular sizes are smaller than 30 arcsec. Higher-resolution MERLIN images are also given for six previously-mapped small sources.

Key words: surveys — galaxies: active — radio continuum: galaxies — radio continuum: general

1. Introduction

At present the only completely identified sample of radio sources is the 3CRR survey (Laing et al. 1983). The parent 3C radio sample has been in existence for nearly 35 years and remains the most important single sample of radio sources. This is because it is (i) complete - it has a flux limit and has virtually complete redshift information - and (ii) unbiased - the sample is selected at low radio frequency, and is therefore not influenced by flat-spectrum components, for which Doppler beaming distorts the statistics by enhancing the flux of radio sources whose axes just happen to be pointing in our direction.

However, it is likely that the 3C sample, although it makes finding galaxies at high redshift easy, is not a representative sample of high-redshift galaxies because the presence of powerful radio AGN affects the properties of the optical galaxy. Specifically, the discovery of UV-optical extended continuum (McCarthy et al. 1987) aligned with the radio axis is evidence for very strong interaction between the radio jet and the intragalactic medium. It has been claimed (Dunlop & Peacock 1993) that this alignment effect tends to disappear at radio powers only a factor $5-10$ lower than the 3C survey. In this case we might expect to pick up passively evolving giant ellipticals by selecting lower-luminosity radio galaxies. There is, however, much debate about this point (e.g. Eales & Rawlings 1996).

These observations are part of an ongoing project (Rhee et al. 1996; hereafter Paper I) to identify and study radio galaxies and quasars from the 4C survey (Pilkington & Scott 1965; Gower et al. 1967) between declinations of $-4°$ and $+4°$. The 4C survey is approximately a factor of 5 deeper than the 3C survey, and has a limiting flux density of 2 Jy at 178 MHz. In order to get a complete sample, large enough to study the properties of distant galaxies, to determine their space density and to be able to compare the properties of the steep spectrum radio galaxies with those of normal radio galaxies and quasars, we selected the 4C sources whose angular sizes are smaller than 30 arcseconds using the 365-MHz Texas survey (Douglas et al. 1980). Our selection is independent of the radio spectral index and the complete radio sample will be published elsewhere. The subset of the 4C sample whose declinations are between $-4°$ and $+4°$ has a lot of radio observations, providing good radio spectral indices and has the advantage of being observable from both hemispheres. In this article, we have concentrated on steep radio spectrum $\alpha > 0.9$[1] objects which are not identified on the Palomar Sky Survey in order to improve positional information for followup optical spectroscopy. The sources have also been selected, as in Paper I, to have angular sizes of less than $30''$. Here we present radio maps of a further 144 radio sources (19 of which are common with Paper I). The sources were chosen as far as possible to complete the mapping of RA ranges according to the LST ranges at which the observations were scheduled. Hence most sources have RA $<$ 5h, 8h $<$ RA $<$ 11h, 15h $<$ RA $<$ 18h and RA $>$ 20h.

[1] The spectral index is defined by Flux Density $\propto$ (Frequency)$^{-\alpha}$.

2. Observations

The observations were performed using the VLA in B-configuration at a frequency centred on 4860.1 MHz, on four occasions: 1994 July 8, 1994 July 30, 1995 October 9 and 1995 December 10. Data were taken in two contiguous bands of 50 MHz bandwidth centred at 4835 MHz and 4885 MHz. Exposure times were 2 minutes, resulting in a theoretical rms noise level of 0.10 mJy/beam; the median noise level of the maps is in fact about 0.1 mJy/beam (estimated from the rms in the bottom 20 pix^2 of each map). Phase calibration was performed typically once every $10-15$ sources using point-source calibrators from the VLA Calibrator List (Perley 1982) during the 1995 observations, although only sporadic phase calibration is available for the 1994 observations. Flux densities were bootstrapped to the source 3C 48, using the value of 5.4 Jy at 4850 MHz from Baars et al. (1979). After calibration in AIPS, the data on each source in turn were mapped using the Caltech Difmap package (Shepherd et al. 1995), typically involving one pass of phase selfcalibration and one of amplitude self-calibration between passes through the CLEAN algorithm, using windows to build up flux in successively fainter parts of the source. A few sources (nearly all of them bright point sources) had residual offset corrections applied in addition. The final dataset was then read back into AIPS and the CLEAN algorithm was applied using the task IMAGR with the ROBUST parameter set to zero, giving a weighting scheme intermediate between natural and uniform weighting. In a few cases the Difmap CLEANed map was used as the final map. The combination of the two algorithms allowed easy interactive investigations of the data combined with deep and thorough CLEANing.

For each component of each object, the peak and extended fluxes have been measured by hand using the AIPS task TVSTAT. This procedure gives an indication of the flux, although it may not be totally reliable in cases where components are not well resolved from each other or when components are large and extended, and hence partially resolved out by the interferometer. Where a core was seen on the map, this was measured separately; otherwise a value is typically quoted for each lobe of a double source. 19 objects overlap with the sample observed in Paper I at 1.4 GHz.

Basic observational parameters are given in Table 1, namely the date of the observation, details of the point-source response in the map, and comments about the data analysis. In Table 2 we present the flux and position measurements for the individual components, and indicate by an asterisk those cases in which the core is likely to be detected (although lacking spectral indices for each component we cannot identify the cores definitely). Figure 1 shows the maps of the sources. The noise level in each observation can be deduced from Fig. 1, in which the lowest contour is 2.8 times the rms noise level. In some cases only point sources are visible. In these cases, however, there is sometimes an indication of further resolved structure which the observations do not have the spatial frequency coverage to map properly.

A few, mostly small, sources were also mapped using the MERLIN interferometer at L-band ($\sim$1.4 GHz). The dates and details of these observations are given in Table 3, and the resulting maps in Fig. 2.

Acknowledgements. The Very Large Array is operated by Associated Universities for Research in Astronomy Inc. under agreement with the National Science Foundation. MERLIN is operated as a National Facility by the University of Manch ester on behalf of the UK Particle Physics and Astronomy Research Council.

References

Baars J.W.M., Genzel R., Pauliny-Toth I.I.K., Witzel A., 1979, A&A 61, 99
Douglas J.N., Bash F., Torrence G., Wolfe C., 1980, Univ. Texas Pub. Astron. 17, 1
Dunlop J.S., Peacock J.A., 1993, MNRAS 263, 936
Eales S.A., Rawlings S., 1996, ApJ 460, 68
Gower J.F.R., Scott P.F., Wills D., 1967, MemRAS 71, 49
Laing R.A., Riley J., Longair M.S., 1983, MNRAS 204, 151
McCarthy P., van Breugel W., Spinrad H., Djorgovski S., 1987, ApJL 321, L29
Perley R.A., 1982, AJ 87, 859
Pilkington J.D.H., Scott P.F., 1965, MemRAS 69, 183
Rhee G., Marvel K., Wilson T., Roland J., Bremer M., Jackson N., Webb J., 1996, ApJS 107, 175 (Paper I)
Shepherd M.C., Pearson T.J., Taylor G.B., 1995, BAAS 27, 903

Table 1. Objects observed, together with the major and minor axis (in arcseconds) and position angle (in degrees) of the restoring beam. Epochs are numbered as follows: 1 = 1994 July 8; 2 = 1994 July 30; 3 = 1995 October 9; 4 = 1995 December 10

IAU name	Epoch	$\theta_{\rm maj}('')$	$\theta_{\rm min}('')$	PA	Comments
0010+005	4	1.54	1.22	−10.34	
0018−012	4	1.47	1.13	−13.35	
0021−031	4	1.52	1.16	−10.43	
0031+010	4	1.41	1.14	−13.70	Two sources?
0043+000	4	1.71	1.30	−16.66	
0105+025	4	1.54	1.21	−20.36	
0109+026	4	1.54	1.24	−18.48	
0111−002	4	1.61	1.25	−17.00	
0115−016	4	1.62	1.23	−18.93	
0117+024	4	1.56	1.23	−19.50	
0119−001	4	1.63	1.24	−17.78	
0119−005	4	1.63	1.22	−17.86	
0119−022	4	1.68	1.23	−20.34	
0131−001	4	1.79	1.45	−38.58	
0132−002	4	1.63	1.24	−20.75	
0140−030	2	2.53	1.28	44.41	
0141−039	2	2.68	1.27	47.04	
0144+037	2	2.29	1.27	49.53	Bad data; confusion?
0144−022	2	2.59	1.27	47.60	
0152+033	2	2.25	1.28	48.15	
0207−018	2	2.33	1.29	44.84	
0211+027	2	2.12	1.31	47.64	
0213−026	2	2.40	1.28	43.82	
0235−019	2	2.18	1.19	41.40	
0300+020	2	1.84	1.29	39.79	
0307+010	2	1.83	1.27	36.38	
0328−032	2	1.92	1.25	29.59	
0355−037	4	2.73	1.23	−47.48	
0358+021	2	1.77	1.23	31.13	
0359+028	2	1.67	1.25	26.81	
0400−031	2	2.27	1.36	34.84	
0407+012	2	1.79	1.24	29.69	
0421+004	2	1.76	1.26	31.34	
0429+025	2	1.66	1.21	27.82	
0449−012	2	1.59	1.27	13.08	Confusing source 35″W, 120″N
0502−023	2	1.66	1.24	13.52	Marginal detection, heavily resolved
0544+013	2	1.56	1.20	16.74	
0815−023	2	1.88	1.28	−31.02	
0819+024	2	1.72	1.28	−34.51	
0825+013	2	1.78	1.27	−33.08	
0836−004	3	1.99	1.29	−23.52	
0844+021	3	1.82	1.29	−21.18	
0852+029	2	1.81	1.26	−40.80	
0856−002	3	1.81	1.22	−22.37	Classical double + point
0857−026	2	2.03	1.30	−38.33	
0906+011	2	1.93	1.34	−42.34	
0915+025	3	1.94	1.26	−43.46	Source may be bandwidth-smeared
0915+025	2	1.94	1.34	−30.18	
0940+001	2	2.09	1.38	−48.78	
0940+012	2	1.93	1.36	−41.31	
0951+009	2	2.22	1.34	−48.14	
0955−014	2	2.30	1.28	−45.89	Bad data
0956−032	2	2.43	1.30	−45.23	Bad data

Table 1. continued

IAU name	Epoch	$\theta_{\rm maj}('')$	$\theta_{\rm min}('')$	PA	Comments
1001−023	2	2.21	1.19	−43.17	Difmap CLEAN map used
1012+022	2	2.30	1.29	−46.52	
1019−009	3	2.68	1.39	−42.63	
1022−020	2	2.55	1.30	−45.82	
1027+008	2	2.28	1.22	−48.58	
1039+019	3	2.53	1.39	−48.33	
1044−008	3	2.66	1.33	−45.07	SE component bandwidth smeared
1044−019	3	2.99	1.40	−45.73	
1046+012	3	2.57	1.32	−46.28	
1049−001	3	2.84	1.40	−47.06	
1052+023	3	2.63	1.44	−49.47	
1500−023	3	1.92	1.26	33.08	
1502+039	3	1.77	1.25	35.91	
1502−001	3	1.84	1.27	34.43	
1509+015	3	1.76	1.22	36.84	
1509−036	3	1.92	1.27	30.86	
1523+033	3	1.72	1.26	32.55	
1523−017	3	1.88	1.26	31.87	
1529+038	3	1.85	1.36	33.47	Heavily resolved extended structure
1536−020	3	1.83	1.28	29.11	
1548+013	3	1.54	1.18	32.30	
1555+016	3	1.60	1.21	29.63	
1603+005	3	1.62	1.22	29.38	
1605−039	3	1.69	1.30	20.49	
1605−041	3	1.81	1.24	24.50	
1608−036	3	1.81	1.26	23.00	
1617+015	3	1.69	1.27	25.53	
1622−035	3	1.74	1.19	24.80	
1627−032	3	1.78	1.27	22.93	
1638−025	3	1.59	1.16	17.27	
1646+003	3	1.69	1.26	18.26	
1650+004	3	1.58	1.20	23.08	
1650−031	3	1.65	1.18	20.02	
1654−020	3	1.70	1.26	21.37	
1658−011	3	1.69	1.24	17.58	
1658−015	3	1.69	1.26	20.81	
1659+010	3	1.59	1.21	22.65	
1704+001	3	1.57	1.21	21.78	
1706−028	3	1.66	1.20	20.87	
1711+006	3	1.66	1.27	18.81	
1714+037	3	1.51	1.21	23.86	
1714−034	3	1.70	1.25	18.54	
1726−038	3	1.75	1.25	15.65	
1735+034	3	1.50	1.19	22.89	
1735−010	3	1.50	1.19	18.21	Core+lobe of large triple?
1748+031	3	1.55	1.27	16.43	
1955+013	1	1.55	1.25	−6.62	Only a few seconds on source
2001−020	4	2.17	1.26	42.81	
2001−022	1	1.63	1.22	−1.80	
2003−025	4	1.56	1.17	1.16	
2018+005	1	1.57	1.23	−2.48	
2020+014	1	1.49	1.18	0.78	
2034+027	1	1.45	1.18	−5.58	
2042+032	1	1.53	1.25	−1.42	
2049+000	1	1.65	1.28	−6.70	

Table 1. continued

IAU name	Epoch	$\theta_{\rm maj}(")$	$\theta_{\rm min}(")$	PA	Comments
2057−041	1	1.65	1.25	−6.91	
2106+032	1	1.47	1.20	−13.88	
2108+039	1	1.42	1.19	−11.35	
2124+012	1	1.50	1.14	−17.68	Marginal detection, heavily resolved
2125+013	1	1.58	1.21	−16.13	
2135+037	1	1.50	1.19	−17.48	
2139+028	1	1.55	1.24	−15.71	
2152+022	1	1.60	1.25	−19.14	
2200+006	1	1.64	1.25	−20.27	
2201+018	1	1.47	1.15	−23.33	
2201−006	4	1.56	1.18	16.65	
2205−040	1	1.74	1.24	−18.55	
2206+038	1	1.61	1.23	−18.25	
2210+016	1	1.52	1.19	−20.54	
2211−035	1	1.71	1.24	−17.25	
2214−035	1	1.67	1.19	−19.72	
2219−030	1	1.67	1.23	−13.26	
2221+025	1	1.54	1.19	−20.21	
2224+006	1	1.42	0.98	−22.41	
2225−019	1	1.69	1.25	−18.40	
2231+015	1	1.54	1.20	−20.70	
2234+009	4	1.52	1.21	9.20	
2238−011	1	1.64	1.17	−22.84	
2241+013	1	1.63	1.26	−23.80	
2247+034	1	1.54	1.15	−24.34	
2250+034	1	1.54	1.17	−23.48	
2252+021	1	1.59	1.16	−22.26	
2304+006	1	1.59	1.20	−25.76	
2305+022	1	1.64	1.24	−26.58	
2309−014	1	1.67	1.23	−24.35	
2330+015	1	1.53	1.17	−31.23	
2334+040	1	1.67	1.24	−31.65	
2335+031	1	1.56	1.27	−33.20	
2347−026	1	1.75	1.24	−32.07	
2354−027	1	1.68	1.20	−30.33	
2356+033	1	1.75	1.25	−31.92	

Table 2. Positions of sources observed with the VLA, together with flux (mJy)es derived from the maps (see text). Both peak and integrated fluxes are given. Probable cores are indicated by an asterisk

4C name	IAU name	RA (1950)	Dec (1950)	$F_{\rm peak}$ (mJy)	$F_{\rm total}$ (mJy)	Angular size ($''$)
4C+00.01	0010+005	00 10 37.41	+00 35 09.2	226.0	451.8	34.3
		00 10 36.71	+00 34 51.2*	1.5	1.6	
		00 10 36.32	+00 34 39.1	10.5	105.8	
4C−01.01	0018−012	00 18 51.71	−01 12 19.0	208.6	357.2	0.0
4C−03.01	0021−031	00 21 02.82	−03 09 44.3	164.1	178.8	0.0
4C+00.04	0031+010	00 31 44.87	+01 03 33.6	8.4	35.6	123.0
		00 31 45.70	+01 03 15.3	8.3	20.1	
		00 31 44.87	+01 02 49.2	1.2	22.1	
		00 31 45.22	+01 02 04.6*	4.3	4.4	
		00 31 45.85	+01 01 31.5	12.9	126.0	
4C−00.05	0043+000	00 43 07.75	+00 04 46.6	62.0	116.8	22.0
		00 43 08.25	+00 04 39.6*	0.9	1.2	
		00 43 08.94	+00 04 33.8	5.2	35.9	
4C+02.02	0105+025	01 05 50.16	+02 33 50.6	12.0	12.7	2.6
		01 05 50.00	+02 33 49.7	48.1	51.6	
4C+02.03	0109+026	01 09 42.39	+02 41 46.1	9.8	46.4	4.9
		01 09 42.29	+02 41 44.1	84.4	171.2	
		01 09 42.35	+02 41 41.2	15.3	33.6	
4C−00.07	0111−002	01 11 56.33	−00 15 07.8	25.5	73.3	18.2
		01 11 55.88	−00 15 14.8*	35.7	39.6	
		01 11 55.36	−00 15 18.8	9.4	50.5	
4C−01.07	0115−016	01 15 42.20	−01 36 16.6	290.8	316.1	0.0
4C+02.05	0117+024	01 17 54.00	+02 27 17.6	68.5	72.8	5.1
		01 17 54.29	+02 27 14.9	1.1	1.8	
4C−00.09A	0119−001	01 19 32.10	−00 06 41.6	35.5	37.9	0.0
4C−00.09B	0119−005	01 19 40.32	−00 33 41.2	248.7	283.5	10.0
		01 19 39.70	−00 33 45.0	7.8	31.6	
4C−02.05	0119−022	01 19 51.07	−02 15 36.6	9.4	22.5	20.0
		01 19 51.63	−02 15 41.5*	0.8	0.9	
		01 19 52.31	−02 15 43.9	93.5	109.1	
4C−00.11A	0131−001	01 31 38.98	−00 11 35.7	457.3	467.2	0.0
4C−00.11B	0132−002	01 32 17.87	−00 13 02.6	23.1	30.9	9.1
		01 32 17.77	−00 13 11.6	37.9	62.7	
4C−03.04A	0140−030	01 40 51.77	−03 02 00.5	72.4	100.8	0.0
4C−03.04B	0141−039	01 41 48.71	−03 54 47.2	50.2	74.3	15.5
		01 41 47.70	−03 54 50.7	16.9	33.2	
4C+03.03	0144+037	01 44 44.37	+03 46 38.3	20.0	73.7	22.3
		01 44 43.51	+03 46 32.5	16.3	20.3	
		01 44 43.01	+03 46 29.3	19.1	78.3	
4C−02.08	0144−022	01 44 20.12	−02 12 19.1	213.6	235.3	0.0
4C+03.04	0152+033	01 52 32.75	+03 23 47.4	53.9	126.0	14.3
		01 52 32.34	+03 23 44.5	6.1	6.7	
		01 52 31.91	+03 23 40.7	131.8	184.6	
4C−01.10	0207−018	02 07 12.41	−01 51 41.3	154.2	180.4	4.6
		02 07 12.70	−01 51 42.8	71.0	91.4	
4C+02.06	0211+027	02 11 10.12	+02 46 25.3	52.2	55.8	12.1
		02 11 09.52	+02 46 17.2	32.4	38.6	
4C−02.09	0213−026	02 13 09.70	−02 36 32.7	4.9	13.0	20.8
		02 13 09.88	−02 36 51.6	590.4	592.8	
		02 13 09.88	−02 36 53.3	29.3	16.6	
4C−02.13	0235−019	02 35 24.69	−01 58 07.0	29.8	93.2	9.2
		02 35 25.23	−01 58 11.3	6.4	23.1	
4C+02.09	0300+020	03 00 23.57	+02 03 45.6	57.9	75.7	5.1
		03 00 23.88	+02 03 43.5	83.3	110.9	
4C+00.12	0307+010	03 07 38.89	+01 01 51.4	19.9	36.5	20.6

Table 2. continued

4C name	IAU name	RA (1950)	Dec (1950)	$F_{\rm peak}$ (mJy)	$F_{\rm total}$ (mJy)	Angular size ($''$)
		03 07 38.10	+01 01 34.6	77.3	109.8	
4C−03.13	0328−032	03 28 41.06	−03 13 23.4	16.3	66.4	20.8
		03 28 42.45	−03 13 23.9	18.9	60.2	
4C−03.15	0355−037	03 55 17.54	−03 42 39.6	27.6	30.0	11.6
		03 55 18.21	−03 42 45.4	14.0	17.7	
4C+02.12	0358+021	03 58 34.24	+02 09 16.2	161.5	222.4	0.0
4C+02.13	0359+028	04 00 00.15	+02 53 47.1	27.1	83.2	24.8
		03 59 59.84	+02 53 32.6*	7.8	9.1	
		03 59 59.43	+02 53 24.8	25.3	85.3	
4C−03.16	0400−031	04 00 44.57	−03 08 09.3	24.1	76.5	24.0
		04 00 43.02	−03 08 15.4	31.7	130.4	
4C+01.08	0407+012	04 07 05.91	+01 17 02.1	18.0	72.3	7.3
		04 07 05.85	+01 16 54.9	59.5	143.1	
4C+00.15	0421+004	04 21 17.31	+00 24 13.4	340.0	350.3	3.2
		04 21 17.15	+00 24 12.2	191.3	287.0	
		04 21 17.36	+00 24 11.6	9.4	17.5	
4C+02.15	0429+025	04 29 40.23	+02 33 38.7	62.8	89.5	5.1
		04 29 40.09	+02 33 34.0	9.6	15.8	
4C−01.14	0449−012	04 49 30.64	−01 17 11.5	46.2	54.7	129.8
		04 49 30.56	−01 17 15.3	47.7	74.6	
		04 49 28.24	−01 19 16.2	10.1	16.9	
4C+01.15	0544+013	05 44 10.83	+01 21 22.3	14.9	25.8	7.9
		05 44 10.50	+01 21 16.2	41.8	53.7	
4C−02.36B	0815−023	08 15 26.15	−02 21 46.3	30.1	48.7	13.7
		08 15 26.48	−02 21 48.7*	3.4	3.9	
		08 15 26.96	−02 21 52.7	34.0	63.9	
4C+02.24	0819+024	08 19 29.57	+02 27 33.4	14.1	26.5	17.5
		08 19 30.11	+02 27 28.5*	2.2	2.2	
		08 19 30.56	+02 27 24.1	18.4	33.6	
4C+01.22	0825+013	08 25 24.82	+01 22 32.2	81.0	105.1	10.4
		08 25 24.98	+01 22 26.7*	0.6	0.5	
		08 25 25.13	+01 22 22.9	51.7	65.1	
4C−00.34	0836−004	08 36 20.74	−00 27 08.3	30.8	100.5	19.3
		08 36 20.34	−00 27 17.3*	2.5	3.1	
		08 36 20.01	−00 27 24.2	18.8	86.9	
4C+02.25A	0844+021	08 44 08.12	+02 11 59.7	11.8	22.8	22.4
		08 44 07.70	+02 11 52.4*	0.5	0.5	
		08 44 07.20	+02 11 42.0	9.5	15.0	
4C+03.14	0852+029	08 52 31.66	+02 56 53.6	88.0	90.1	1.5
		08 52 31.60	+02 56 52.4	123.9	130.1	
4C−00.35	0856−002	08 56 09.05	−00 15 59.6	8.1	49.4	37.9
		08 56 08.16	−00 16 11.4	15.2	70.6	
		08 56 07.25	−00 16 26.2	2.5	3.2	
4C−02.37	0857−026	08 57 22.51	−02 40 48.9	19.6	74.1	23.6
		08 57 22.70	−02 40 57.3	2.9	3.1	
		08 57 23.11	−02 41 10.7	4.3	49.4	
4C+01.24A	0906+011	09 06 33.31	+01 06 54.0	86.2	98.1	6.0
		09 06 33.70	+01 06 52.8	55.1	66.8	
4C+02.26	0915+025	09 15 06.34	+02 31 54.5	13.7	18.7	4.7
		09 15 06.46	+02 31 50.2	14.4	20.4	
4C+02.26	0915+025	09 15 06.34	+02 31 54.8	13.4	19.7	4.9
		09 15 06.46	+02 31 50.2	15.1	23.0	
4C+00.30	0940+001	09 40 45.48	+00 09 21.0*	386.6	398.4	9.1
		09 40 44.94	+00 09 25.1	1.6	1.9	
4C+01.26	0940+012	09 40 47.05	+01 17 28.7	12.4	33.2	127.1

Table 2. continued

4C name	IAU name	RA (1950)	Dec (1950)	$F_{\rm peak}$ (mJy)	$F_{\rm total}$ (mJy)	Angular size ($''$)
		09 40 43.99	+01 16 50.2	1.0	0.9	
		09 40 41.67	+01 16 22.3	11.0	28.2	
		09 40 47.40	+01 15 21.7	6.1	6.3	
4C+00.33	0951+009	09 51 49.51	+00 58 04.2	14.1	40.6	5.1
		09 51 49.23	+00 58 01.3	27.5	31.5	
4C−01.20	0955−014	09 55 55.97	−01 25 36.8	386.3	455.9	0.0
4C−03.39	0956−032	09 56 33.71	−03 12 18.3	11.8	29.4	6.8
		09 56 34.14	−03 12 20.6	33.4	123.6	
4C−02.39	1001−023	10 01 43.29	−02 23 16.6	27.2	54.0	60.2
		10 01 41.22	−02 24 08.2	7.7	31.2	
4C+02.30	1012+022	10 12 40.80	+02 13 50.1	51.5	56.5	8.5
		10 12 41.18	+02 13 49.5	157.0	173.3	
		10 12 40.62	+02 13 48.4	39.4	43.4	
4C−00.38	1019−009	10 19 26.55	−00 54 53.2*	130.4	140.7	0.0
4C−01.22	1022−020	10 22 56.10	−02 02 16.7	28.4	53.8	24.8
		10 22 57.66	−02 02 25.1	30.5	63.1	
4C+00.35	1027+008	10 27 35.82	+00 53 06.2	124.9	208.7	4.9
		10 27 35.82	+00 53 01.3	80.1	168.5	
4C+03.18	1039+029	10 39 04.27	+02 58 16.4	457.2	524.0	5.7
		10 39 04.12	+02 58 14.7	64.2	69.9	
		10 39 04.04	+02 58 11.8	184.9	318.5	
4C−02.42	1044−019	10 44 03.78	−01 57 03.1	2.6	3.2	32.9
		10 44 03.45	−01 57 35.6	24.3	27.2	
4C−00.39	1044−008	10 44 46.60	−00 49 19.5	5.1	106.4	118.6
		10 44 48.43	−00 49 57.5	6.2	6.5	
		10 44 50.56	−00 51 02.2	12.7	55.2	
4C+01.27	1046+012	10 46 21.84	+01 16 09.6	43.9	66.9	4.1
		10 46 21.72	+01 16 05.9	24.6	34.9	
4C−00.40	1049−001	10 49 19.16	−00 09 42.5	95.1	103.1	7.8
		10 49 18.72	−00 09 46.6	29.8	43.4	
4C+02.31	1052+023	10 52 43.89	+02 21 47.6	26.6	56.1	33.0
		10 52 42.77	+02 21 45.9*	49.1	50.2	
		10 52 41.70	+02 21 44.5	50.7	85.7	
4C−02.62	1500−023	15 00 58.90	−02 18 48.7	332.8	348.6	0.0
4C+03.31	1502+039	15 02 36.01	+03 58 47.9	80.0	116.5	0.0
4C−00.58	1502−001	15 02 59.53	−00 06 07.6	260.2	344.6	0.0
4C−03.54	1509−036	15 09 05.92	−03 36 25.9	28.5	72.2	34.0
		15 09 03.77	−03 36 36.6	5.7	42.5	
4C+01.42	1509+015	15 09 53.05	+01 32 24.1	326.6	467.4	7.1
		15 09 52.81	+01 32 18.0	144.7	250.2	
4C+03.33	1523+033	15 23 18.12	+03 18 54.8	689.1	712.5	0.0
4C−01.37	1523−017	15 23 55.35	−01 43 43.1	46.8	104.7	11.3
		15 23 55.60	−01 43 47.2*	5.0	6.7	
		15 23 55.85	−01 43 51.5	62.3	113.6	
4C+03.34	1529+038	15 29 36.59	+03 52 09.6	1.6	33.4	23.4
		15 29 36.17	+03 52 05.5	20.8	22.6	
		15 29 35.31	+03 51 56.2	0.7	20.5	
4C−02.64	1536−020	15 36 25.96	−02 01 31.6	39.2	96.1	35.0
		15 36 26.22	−02 02 06.4	6.8	48.7	
4C+01.46	1548+013	15 48 03.08	+01 21 03.3	3.5	7.0	32.5
		15 48 04.18	+01 20 54.9*	4.0	3.7	
		15 48 05.03	+01 20 49.1	81.4	130.5	
4C+01.47	1555+016	15 55 20.40	+01 41 19.3	79.0	102.8	0.0
4C+00.58A	1603+005	16 03 13.57	+00 34 01.3	133.4	173.6	12.5
		16 03 12.87	+00 33 54.6	98.5	171.5	

Table 2. continued

4C name	IAU name	RA (1950)	Dec (1950)	$F_{\rm peak}$ (mJy)	$F_{\rm total}$ (mJy)	Angular size ($''$)
4C−03.56A	1605−041	16 05 22.84	−04 07 55.8	17.3	25.9	11.2
		16 05 23.03	−04 08 01.0*	0.3	0.4	
		16 05 23.28	−04 08 04.8	35.6	43.6	
4C−03.56B	1605−039	16 05 40.42	−03 52 43.6	5.2	16.4	214.3
		16 05 40.83	−03 52 55.5	10.0	31.9	
		16 05 53.52	−03 54 09.5	21.8	31.6	
4C−03.57	1608−036	16 08 27.86	−03 37 46.2	9.1	31.0	38.5
		16 08 28.05	−03 38 01.8*	1.5	1.4	
		16 08 27.93	−03 38 24.7	2.3	17.9	
4C+01.50	1617+015	16 17 23.98	+01 36 08.0	8.2	29.2	28.6
		16 17 24.35	+01 35 39.9	27.0	63.1	
4C−03.58	1622−035	16 22 32.58	−03 31 51.1	22.3	34.7	0.0
4C−03.60	1627−032	16 27 44.26	−03 15 29.6	3.5	3.8	52.3
		16 27 47.72	−03 15 36.2	37.2	66.7	
4C−02.69	1638−025	16 38 03.21	−02 33 56.8	395.2	561.6	65.4
		16 38 04.06	−02 35 00.9	7.2	9.7	
4C+00.59	1646+003	16 46 52.72	+00 20 20.5	28.9	89.1	8.7
		16 46 52.42	+00 20 13.0	59.8	143.7	
4C−02.71	1650−031	16 50 02.83	−03 07 10.6	118.3	128.5	0.0
4C+00.60	1650+004	16 50 25.02	+00 24 01.2	180.2	177.8	1.8
		16 50 25.04	+00 24 03.0	219.7	193.3	
4C−01.39	1654−020	16 54 20.20	−02 02 09.4	3.1	4.8	5.1
		16 54 20.01	−02 02 11.7	382.8	418.1	
		16 54 19.91	−02 02 12.0	47.7	40.8	
4C−01.40A	1658−015	16 58 30.72	−01 33 36.0	6.6	11.2	0.0
4C−01.40B	1658−011	16 58 32.91	−01 07 59.5	13.3	31.9	14.4
		16 58 32.19	−01 08 09.1	10.8	10.8	
4C+00.62	1659+010	16 59 23.44	+01 04 01.2	136.8	141.4	0.0
4C+00.64	1704+001	17 04 49.19	+00 06 59.7	163.9	239.1	0.0
4C−02.72	1706−028	17 06 12.45	−02 52 14.5	57.9	95.7	5.3
		17 06 12.76	−02 52 17.1	47.4	74.6	
4C+00.66	1711+006	17 11 34.50	+00 38 36.0	28.0	84.9	15.5
		17 11 34.61	+00 38 27.6*	13.3	16.1	
		17 11 34.83	+00 38 21.3	225.9	295.3	
4C−03.63	1714−034	17 14 11.58	−03 29 51.9	6.3	43.3	6.8
		17 14 11.89	−03 29 56.9	45.4	112.4	
4C+03.36	1714+037	17 14 49.89	+03 43 23.2	115.5	174.2	0.0
4C−03.64	1726−038	17 26 12.82	−03 48 17.2	51.9	125.0	23.8
		17 26 12.03	−03 48 28.8*	275.7	287.8	
		17 26 11.68	−03 48 33.8	20.4	125.8	
4C−00.69	1735−010	17 35 08.92	−00 59 49.2	83.6	91.4	86.3
		17 35 10.64	−01 01 11.6	12.6	86.4	
4C+03.37	1735+034	17 35 20.81	+03 27 19.6	67.2	86.9	3.3
		17 35 20.75	+03 27 16.4	368.6	396.1	
4C+03.38	1748+031	17 48 07.87	+03 11 30.8	158.9	292.7	25.8
		17 48 08.45	+03 11 06.5	61.3	165.4	
4C+01.62	1955+013	19 55 20.33	+01 20 27.0	13.9	24.3	0.0
4C−02.78A	2001−020	20 01 44.04	−02 03 47.0	45.3	73.3	18.6
		20 01 43.40	−02 04 02.9	3.5	18.8	
4C−02.78B	2001−022	20 01 53.30	−02 17 39.4	23.1	59.7	10.2
		20 01 53.27	−02 17 43.2*	100.7	111.0	
		20 01 53.19	−02 17 49.5	76.8	117.2	
4C−02.79	2003−025	20 03 32.25	−02 32 14.4	991.2	1060.0	0.0
4C+00.77	2018+005	20 18 29.60	+00 35 13.6	19.0	25.4	14.0
		20 18 29.11	+00 35 10.1*	0.9	0.8	

Table 2. continued

4C name	IAU name	RA (1950)	Dec (1950)	$F_{\rm peak}$ (mJy)	$F_{\rm total}$ (mJy)	Angular size ($''$)
		20 18 28.75	+00 35 07.8	107.5	150.7	
4C+01.63	2020+014	20 20 49.61	+01 26 45.0	102.4	110.7	1.8
		20 20 49.53	+01 26 43.6	11.9	10.2	
4C+02.51	2034+027	20 34 03.72	+02 46 27.5	17.2	21.1	3.0
		20 34 03.60	+02 46 25.1	36.4	38.9	
4C+03.48	2042+032	20 42 51.56	+03 13 40.3	48.2	56.9	18.9
		20 42 51.46	+03 13 30.2*	1.0	1.3	
		20 42 51.30	+03 13 21.8	18.5	37.7	
4C−00.76	2049+000	20 49 30.77	+00 02 07.4	22.1	46.7	13.5
		20 49 30.58	+00 01 59.6*	11.6	12.0	
		20 49 30.48	+00 01 54.6	21.5	41.5	
4C−03.73	2057−041	20 57 57.34	−04 07 04.1	26.2	29.1	0.0
4C+03.49	2106+032	21 06 50.70	+03 14 39.0	48.8	75.5	0.0
4C+03.50	2108+039	21 08 40.26	+03 58 43.8	80.7	83.1	1.3
		21 08 40.30	+03 58 42.6	111.7	106.5	
4C+01.65A	2124+012	21 24 52.49	+01 13 09.5	2.1	57.4	0.0
4C+01.65B	2125+013	21 25 50.79	+01 22 33.4	6.8	32.2	11.7
		21 25 50.77	+01 22 29.0	7.8	8.0	
		21 25 50.56	+01 22 26.4	3.4	4.1	
		21 25 50.29	+01 22 24.4	1.9	4.6	
4C+03.51	2135+037	21 35 30.72	+03 45 29.7	37.3	42.1	0.0
4C+02.53	2139+028	21 39 39.11	+02 48 52.2	33.0	80.8	21.9
		21 39 39.67	+02 48 45.5*	44.0	44.7	
		21 39 40.19	+02 48 37.4	171.7	272.8	
4C+01.67	2152+022	21 52 31.56	+02 12 59.1	14.7	22.0	12.9
		21 52 32.27	+02 12 51.9	49.2	59.3	
4C+00.80	2200+006	22 00 14.75	+00 41 32.6	39.6	41.9	3.0
		22 00 14.81	+00 41 29.7	37.7	39.1	
4C+01.68	2201+018	22 01 14.97	+01 50 26.1	10.1	113.2	40.8
		22 01 14.85	+01 50 12.5*	1.0	1.1	
		22 01 14.68	+01 49 45.5	1.6	9.5	
4C−00.79	2201−006	22 01 24.26	−00 36 21.7	153.9	204.1	0.0
4C−03.76	2205−040	22 05 32.64	−04 02 45.2	14.4	17.8	28.4
		22 05 30.78	−04 02 50.7	29.9	39.0	
4C+03.53	2206+038	22 06 47.21	+03 48 11.2	10.6	23.4	0.0
4C+01.69	2210+016	22 10 05.20	+01 37 59.2	1118.1	1118.5	0.0
4C−03.77	2211−035	22 11 58.16	−03 32 54.1	83.0	142.0	19.6
		22 11 58.43	−03 33 13.3	42.8	102.4	
4C−03.78	2214−035	22 14 38.19	−03 34 57.3	134.9	141.6	3.3
		22 14 37.97	−03 34 57.3	34.0	35.8	
4C−03.80	2219−030	22 19 47.00	−03 05 18.7	305.1	486.2	0.0
4C+02.55	2221+025	22 21 36.78	+02 31 35.7	8.5	11.8	6.6
		22 21 37.11	+02 31 31.3	59.8	69.7	
4C+00.81	2224+006	22 24 13.17	+00 36 52.9	540.7	559.2	0.0
4C−02.85	2225−019	22 25 41.19	−01 58 34.6	22.3	63.1	25.2
		22 25 41.44	−01 58 59.5	41.9	116.6	
4C+01.71	2231+015	22 31 12.31	+01 35 01.4	41.2	45.5	6.1
		22 31 12.31	+01 34 55.3	22.9	33.2	
4C+00.82	2234+009	22 34 01.37	+00 59 01.8	1.8	4.8	10.5
		22 34 00.98	+00 58 53.1	24.4	34.9	
4C−01.58A	2238−011	22 38 24.07	−01 09 16.9	59.9	75.7	8.3
		22 38 24.18	−01 09 21.3	5.9	6.1	
		22 38 24.20	−01 09 25.0	14.6	24.9	
4C+01.72	2241+013	22 41 16.57	+01 20 45.6	20.1	77.7	17.6
		22 41 16.74	+01 20 40.1	12.8	16.7	

Table 2. continued

4C name	IAU name	RA (1950)	Dec (1950)	$F_{\rm peak}$ (mJy)	$F_{\rm total}$ (mJy)	Angular size ($''$)
		22 41 17.17	+01 20 30.5	6.9	38.5	
4C+03.54	2247+034	22 47 46.28	+03 24 10.9	24.9	39.8	0.0
4C+03.55	2250+034	22 50 11.65	+03 28 38.3	140.8	149.1	0.0
4C+02.56	2252+021	22 52 21.09	+02 09 21.8	125.1	154.8	6.8
		22 52 21.25	+02 09 15.4	12.1	23.3	
4C+00.84	2304+006	23 04 09.11	+00 40 36.7	118.9	163.5	8.7
		23 04 09.32	+00 40 28.6	6.1	7.7	
4C+02.57	2305+022	23 05 43.16	+02 12 40.8	50.4	91.8	11.6
		23 05 43.62	+02 12 31.5	35.3	95.7	
4C−01.60	2309−014	23 09 48.31	−01 25 44.4	147.8	166.6	8.8
		23 09 48.09	−01 25 52.6	3.1	5.6	
4C+01.75B	2330+015	23 30 44.23	+01 34 02.4	11.1	50.6	46.0
		23 30 42.29	+01 33 47.6	1.2	20.9	
		23 30 41.48	+01 33 42.1	2.8	7.8	
4C+03.58	2334+040	23 34 32.75	+04 00 01.4	2.8	43.9	23.7
		23 34 33.51	+03 59 55.3	8.4	9.0	
		23 34 34.28	+03 59 55.6	23.1	84.1	
4C+03.59	2335+031	23 35 34.31	+03 10 11.2	396.1	567.2	0.0
4C−02.90	2347−026	23 47 51.49	−02 41 24.8	472.9	503.4	0.0
4C−02.91	2354−027	23 54 32.39	−02 43 01.0*	9.4	10.2	20.7
		23 54 31.91	−02 43 20.4	182.3	226.1	
4C+03.61	2356+033	23 56 09.07	+03 20 28.5	12.3	40.0	14.8
		23 56 08.89	+03 20 21.6*	3.7	3.6	
		23 56 08.74	+03 20 14.6	9.8	44.8	

Table 3. Log of the MERLIN observations

4C name	IAU name	Obs. date	Obs. time (hr)	Frequency (MHz)
4C+00.15	0421+004	1997 May 14	4.1	1658
4C+03.14	0852+029	1997 Mar 30	7.2	1420
4C+00.31	0945+003	1997 Apr 17	8.4	1658
4C−02.63	1509−023	1997 Mar 26	8.0	1658
4C−03.65	1738−033	1997 May 14	8.3	1658
4C+00.80	2200+006	1997 Apr 17	8.0	1420

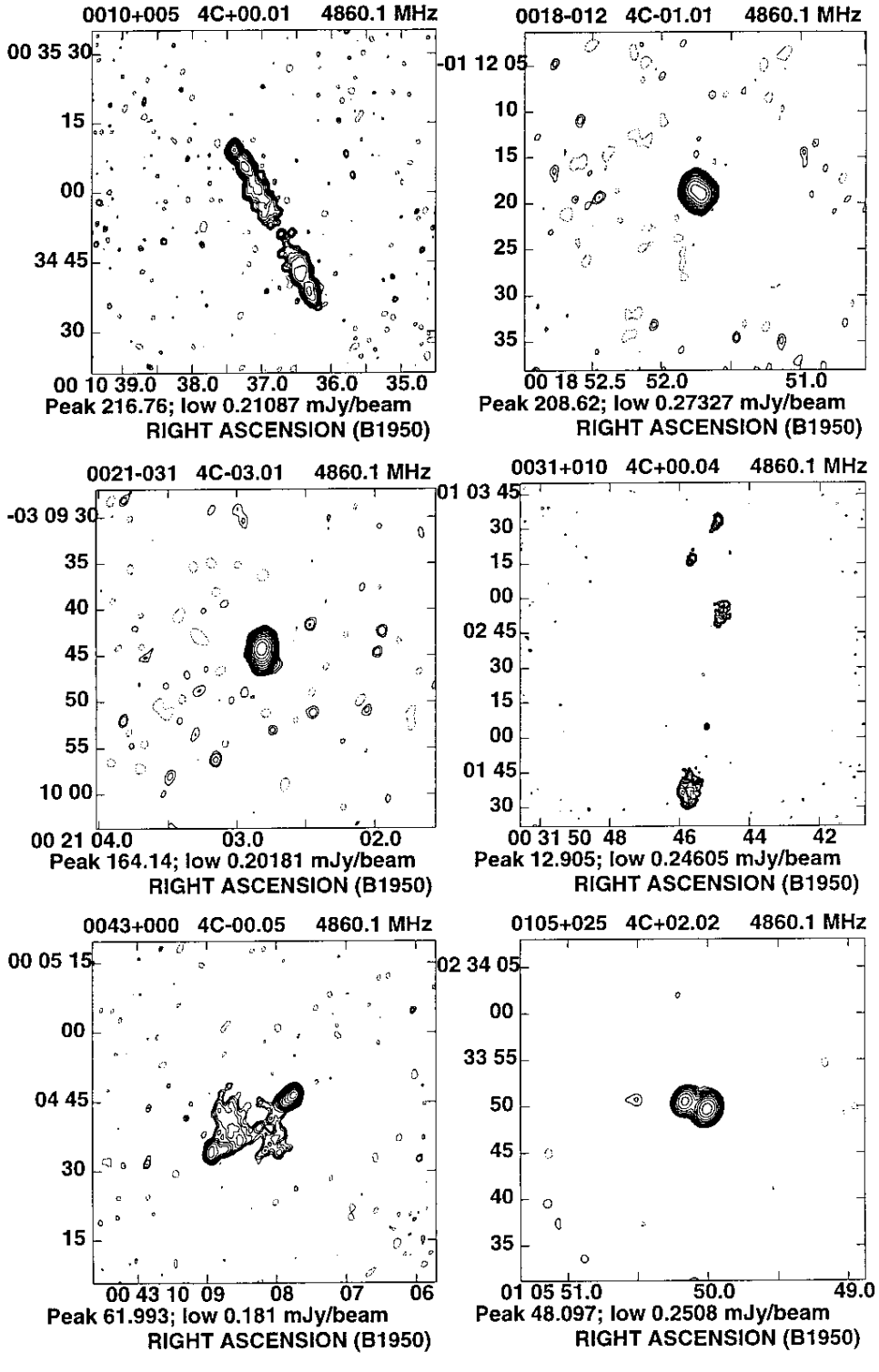

Fig. 1. VLA maps of the sources observed. The bottom contour is indicated on the map (in mJy) in each case, and is always 2.8 times the rms noise level. The contour levels are (−1, 1, 1.4, 2.03, 3.05, 4.7, 7.6, 12.5, 21.2, 37, 67, 123, 235 , 457, 915, 1880, 4000) times the bottom contour

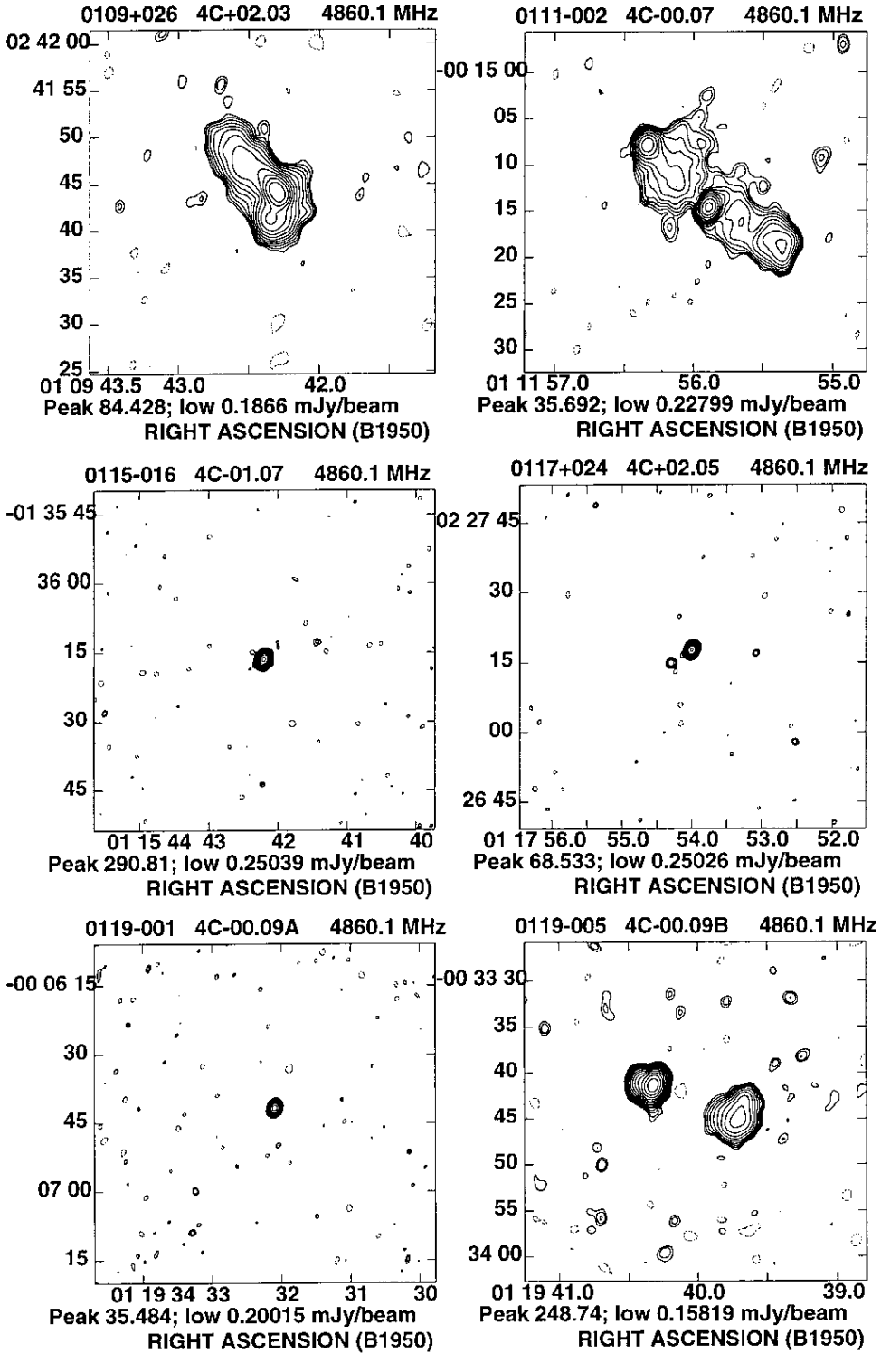

Fig. 1. continued

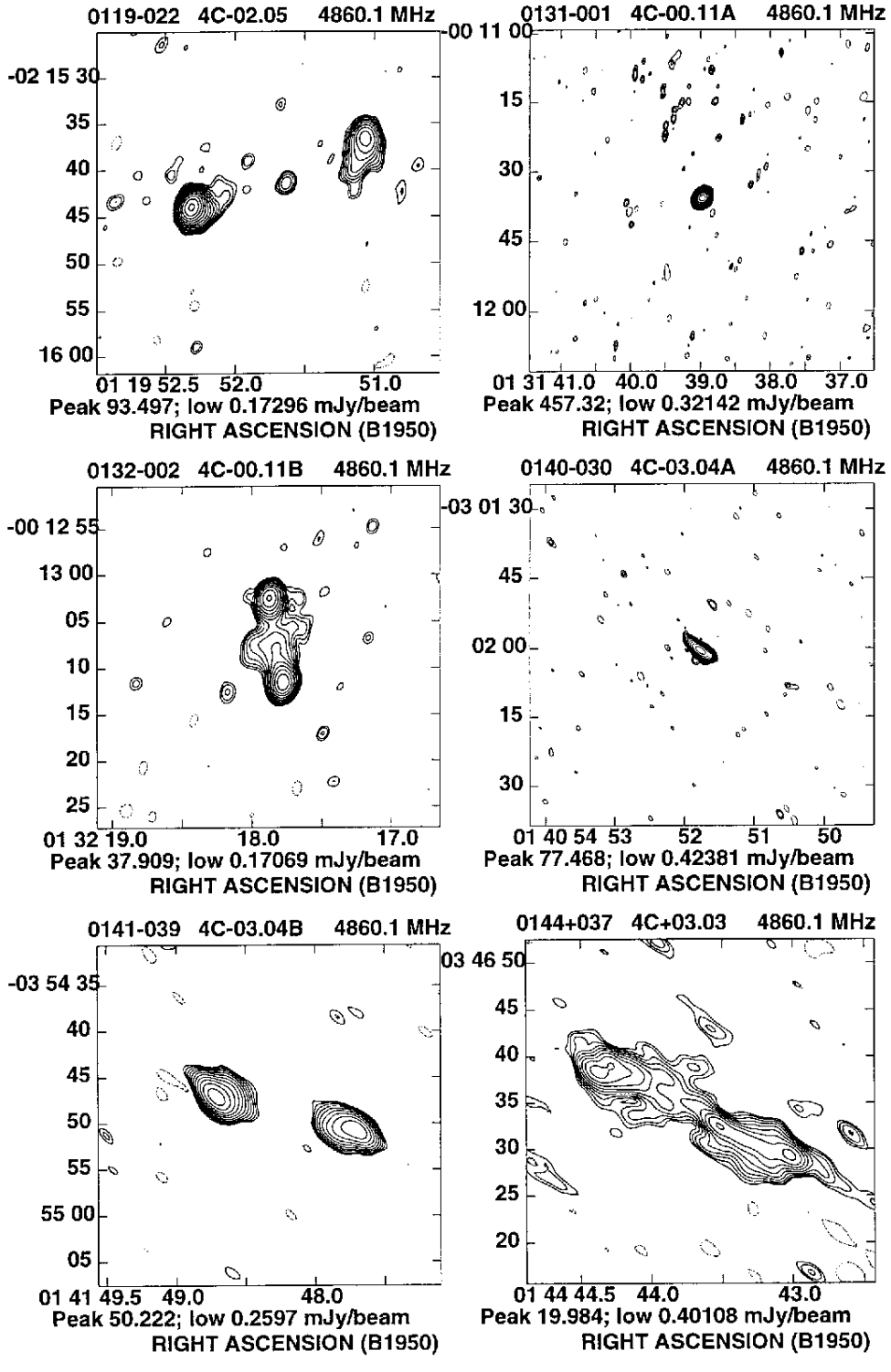

Fig. 1. continued

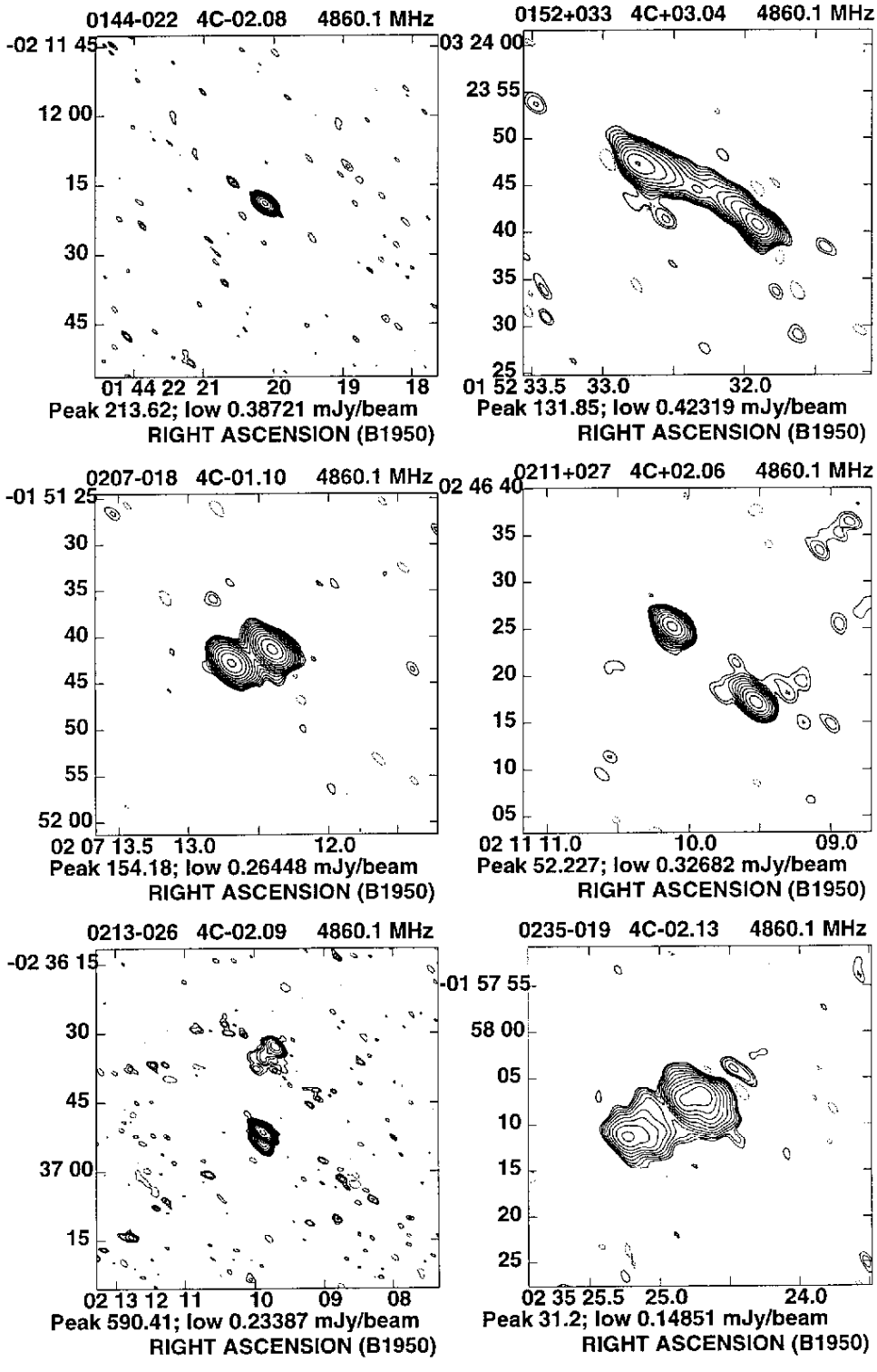

Fig. 1. continued

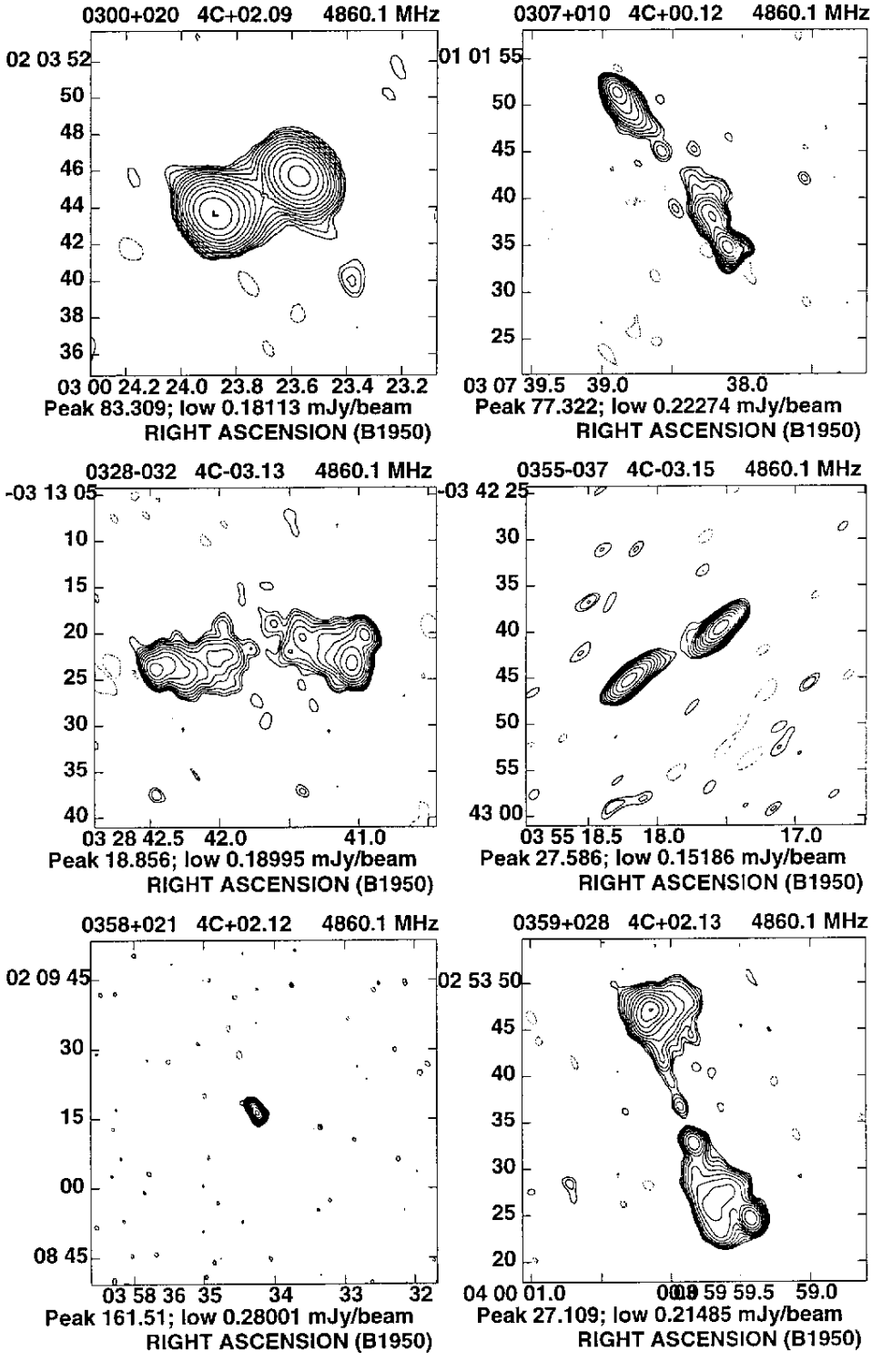

Fig. 1. continued

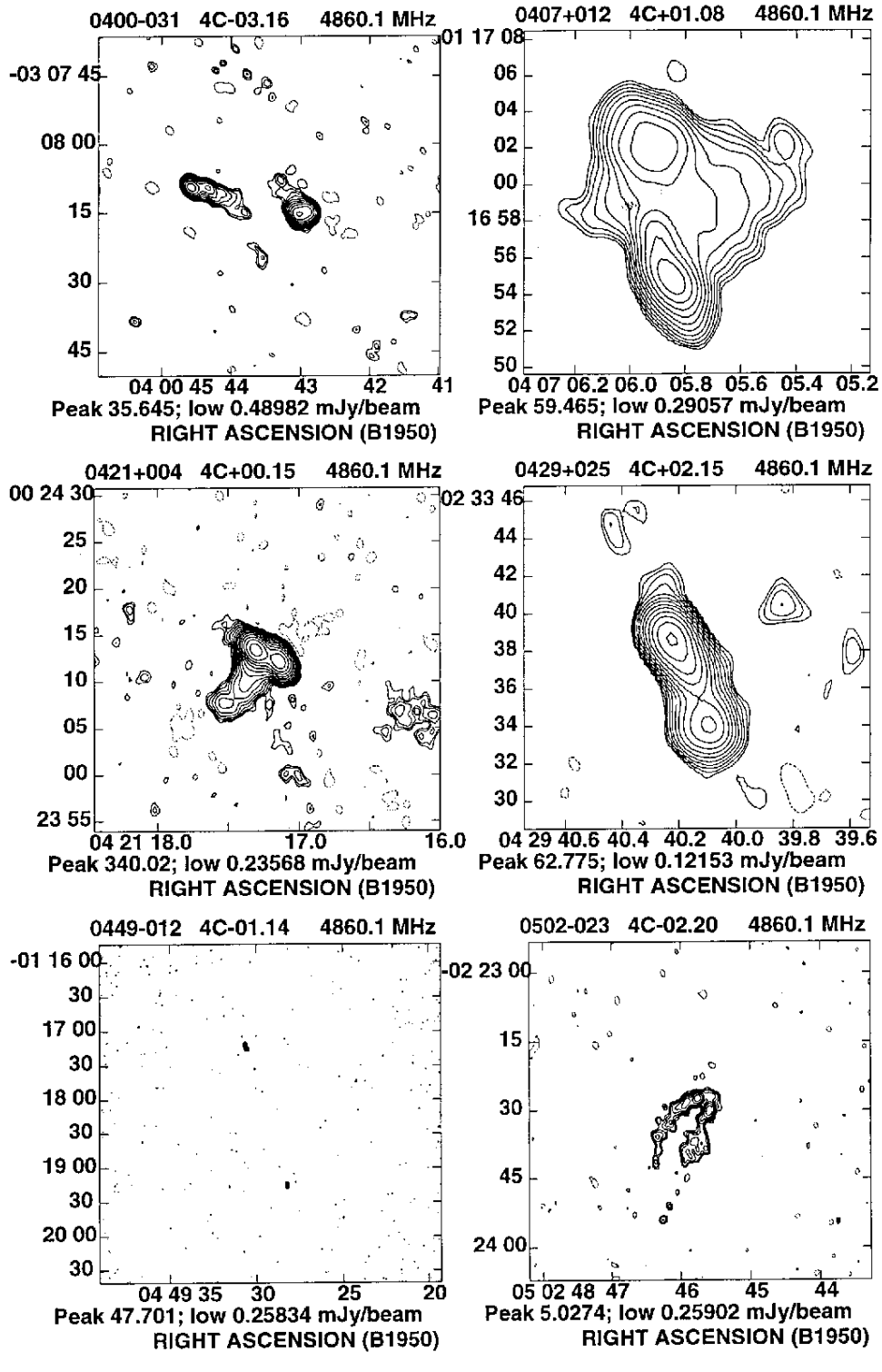

Fig. 1. continued

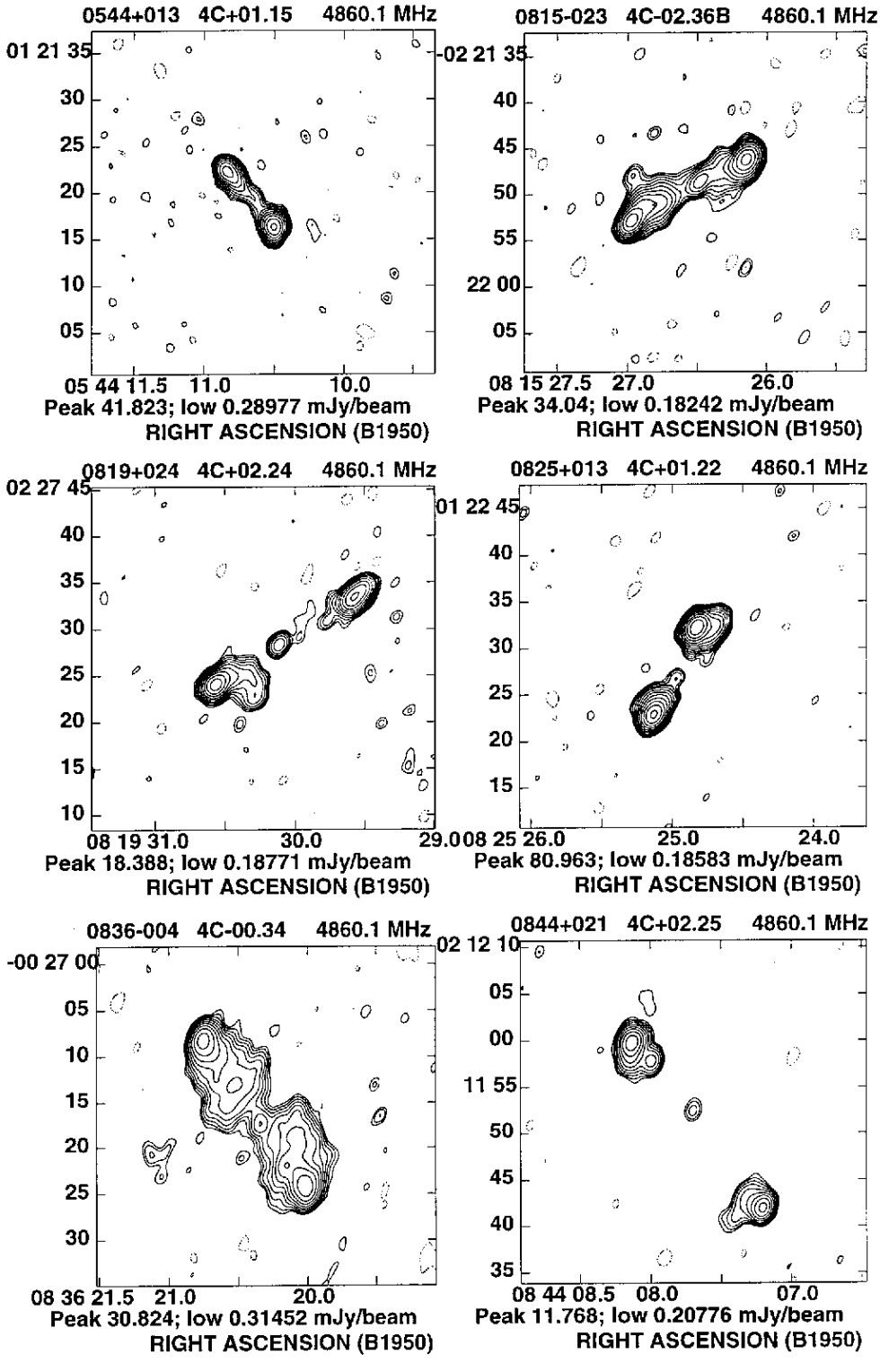

Fig. 1. continued

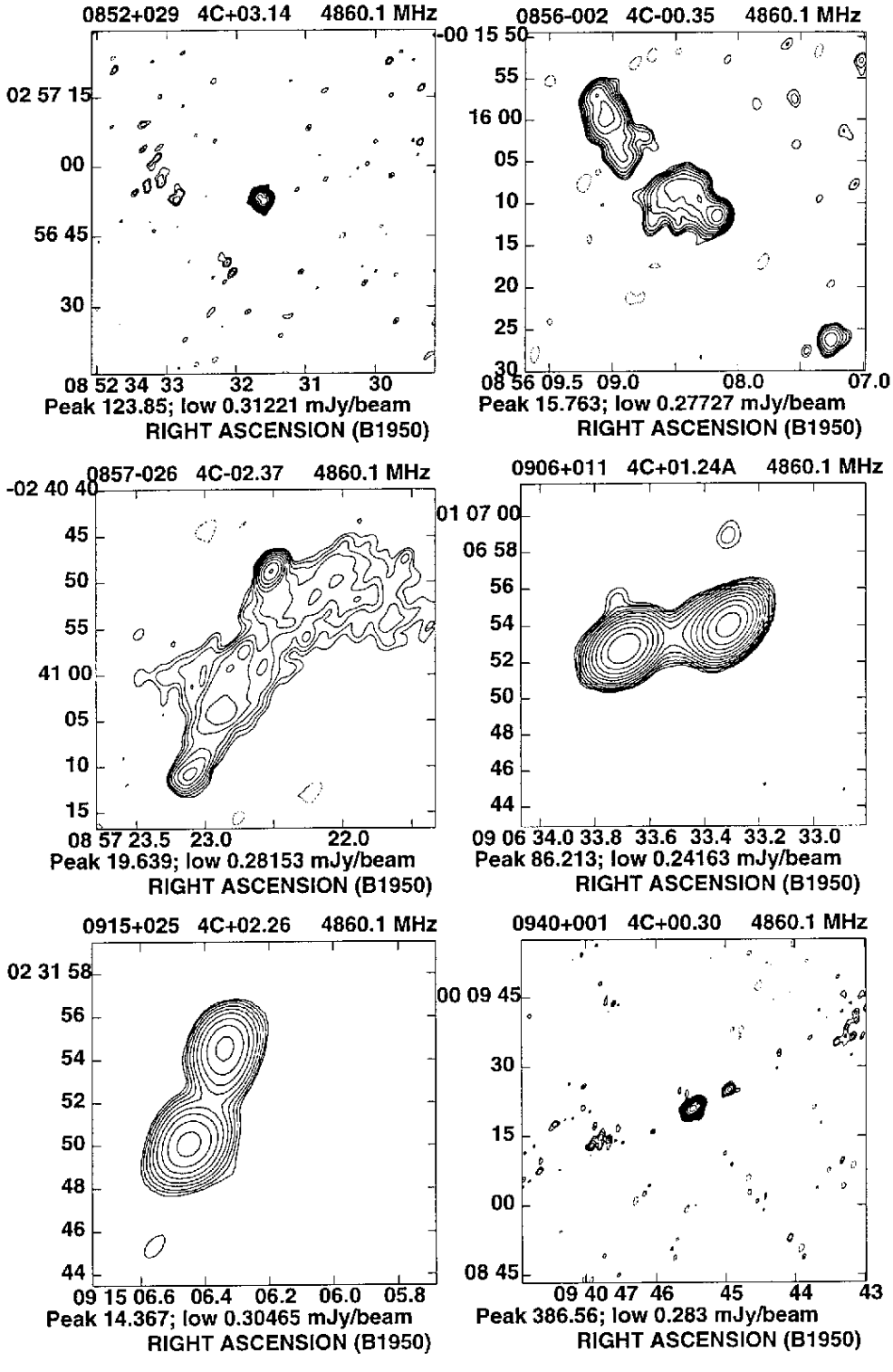

Fig. 1. continued

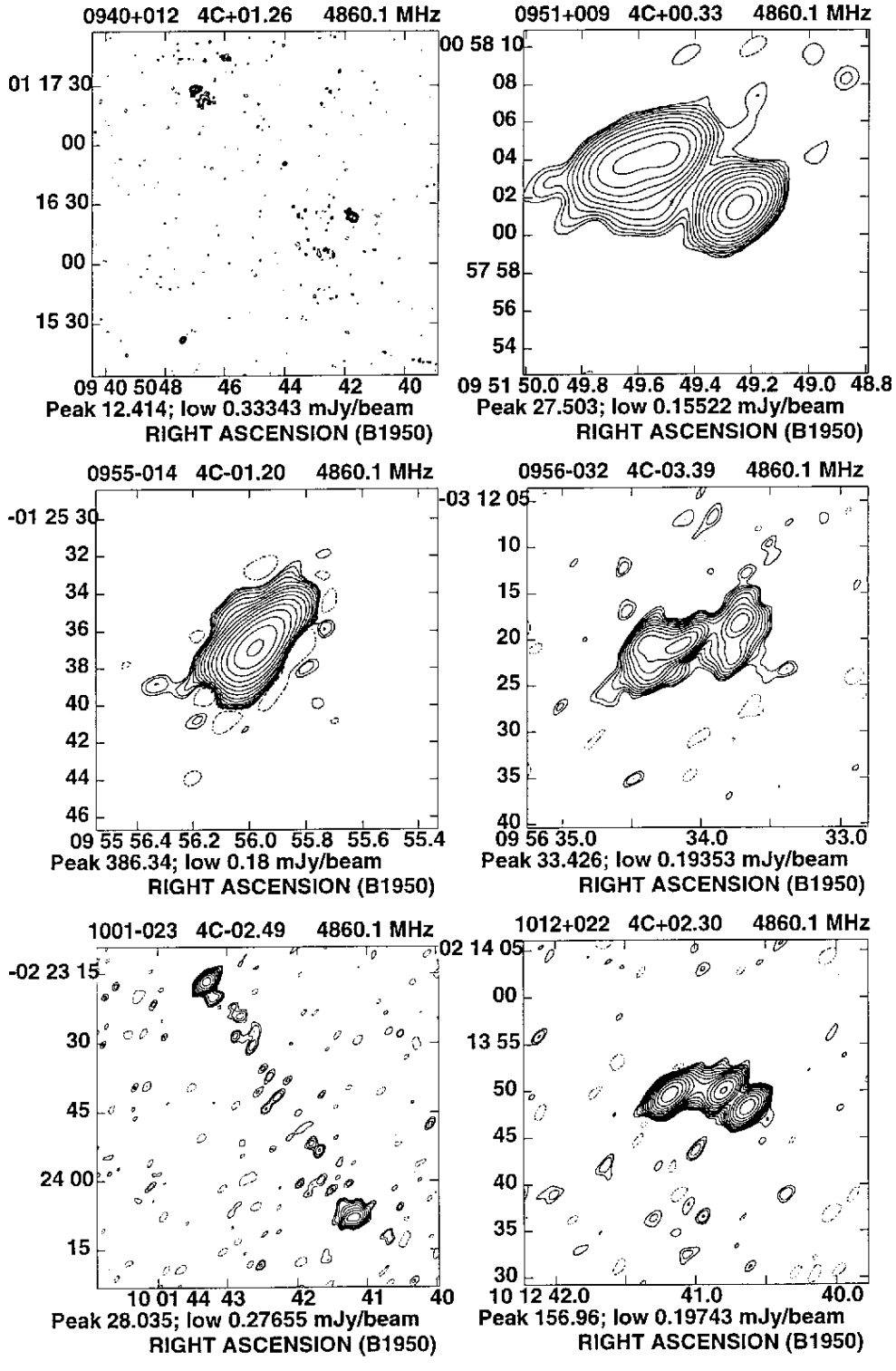

Fig. 1. continued

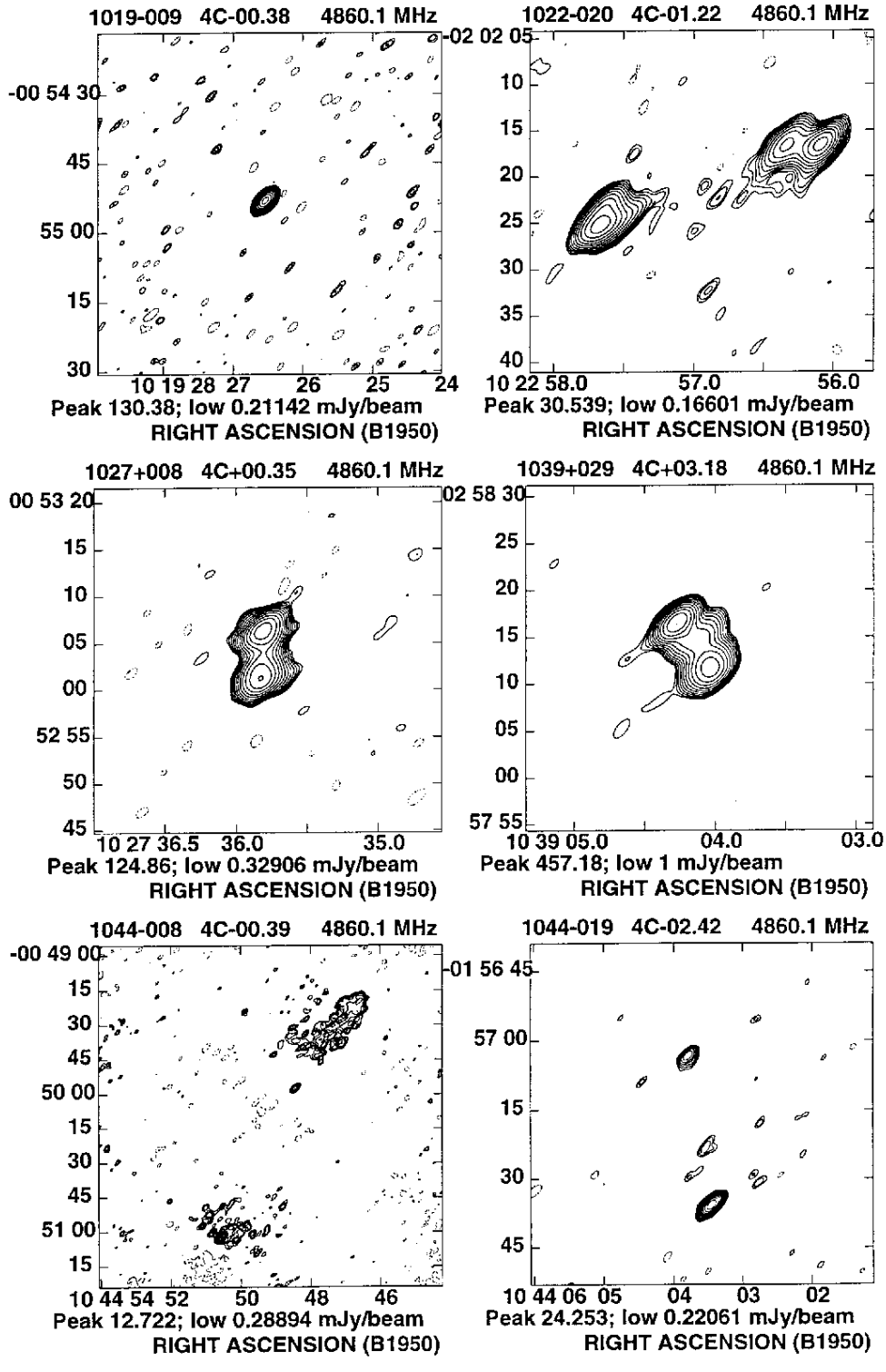

Fig. 1. continued

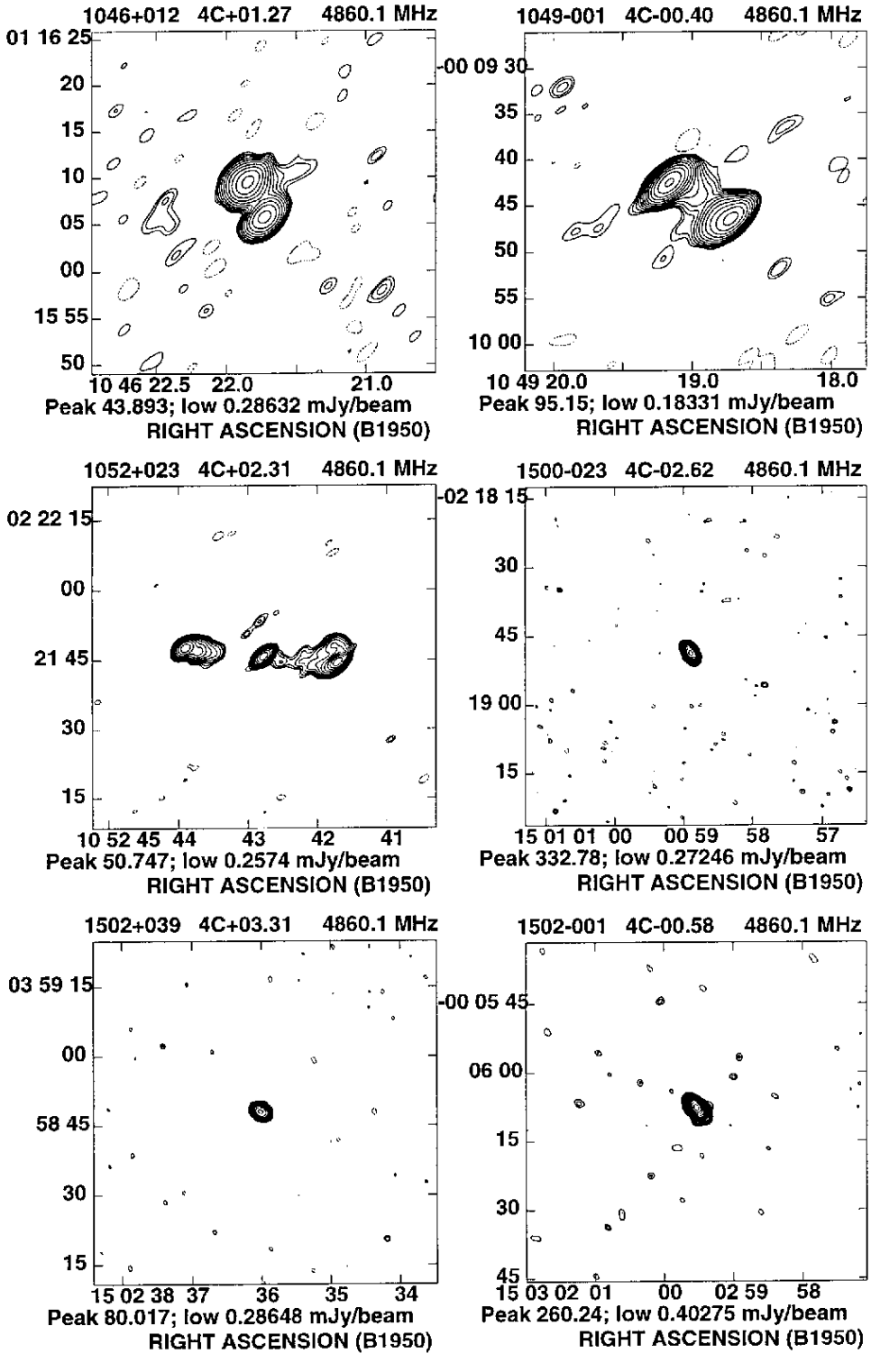

Fig. 1. continued

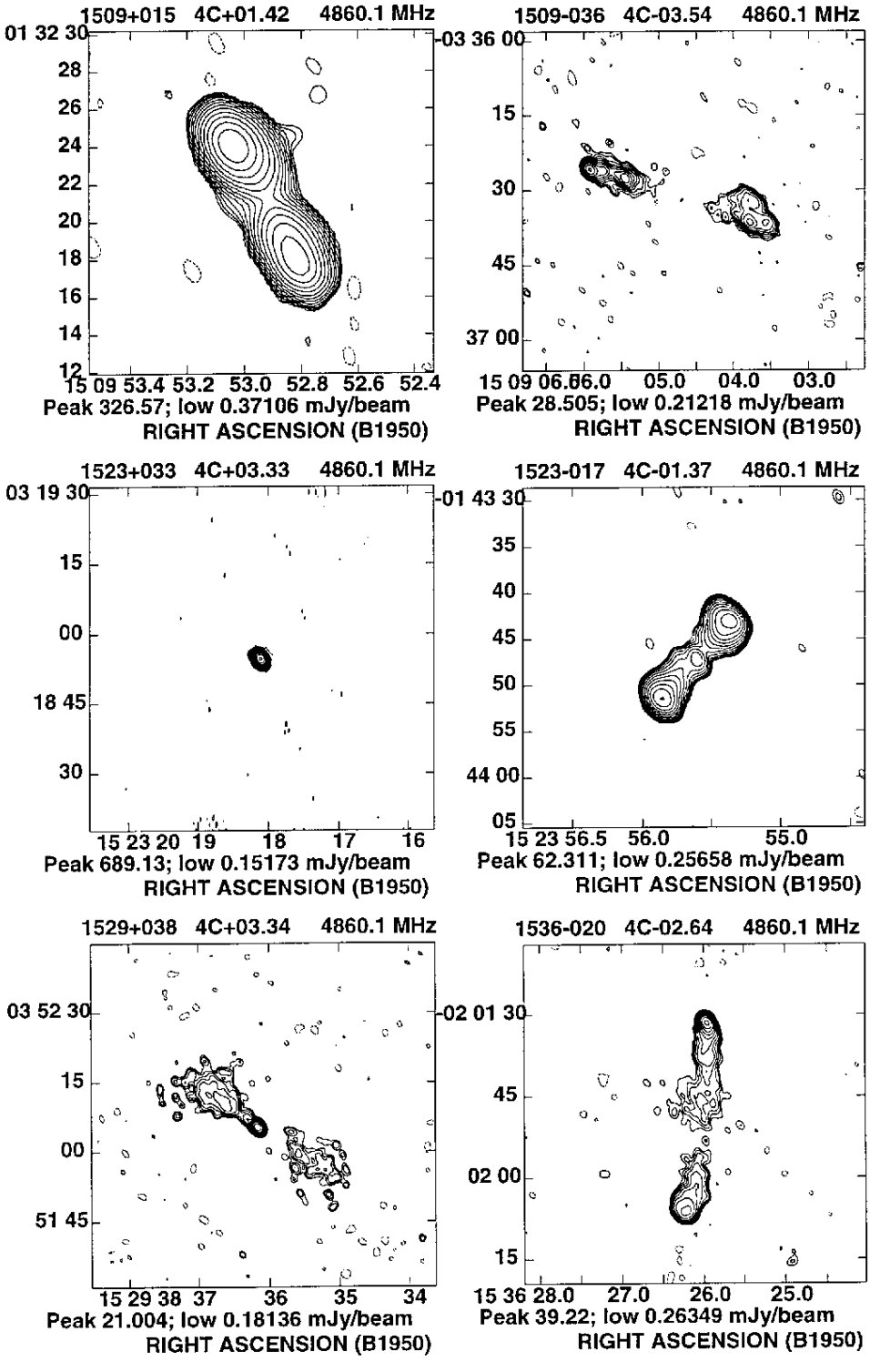

Fig. 1. continued

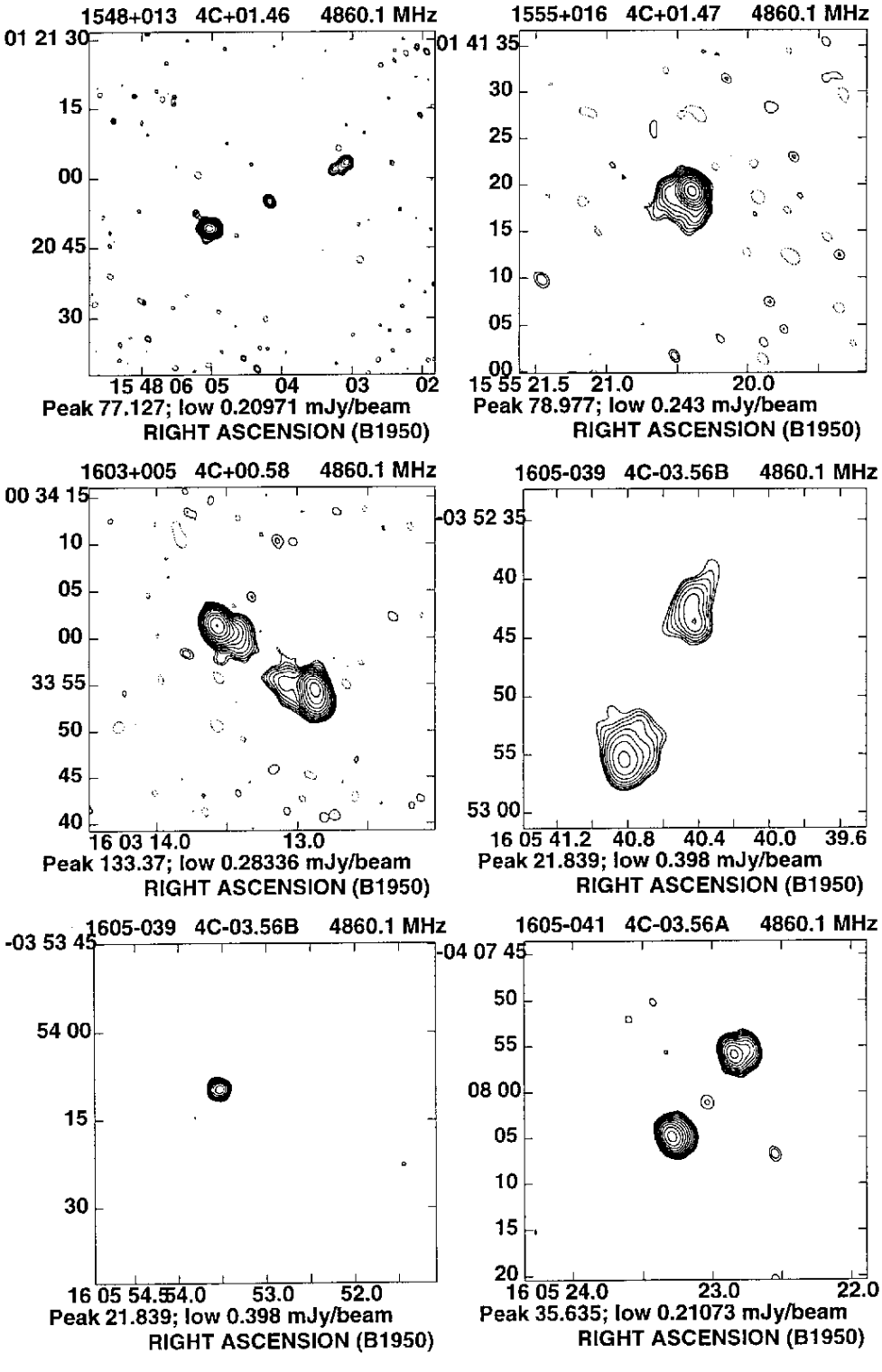

Fig. 1. continued

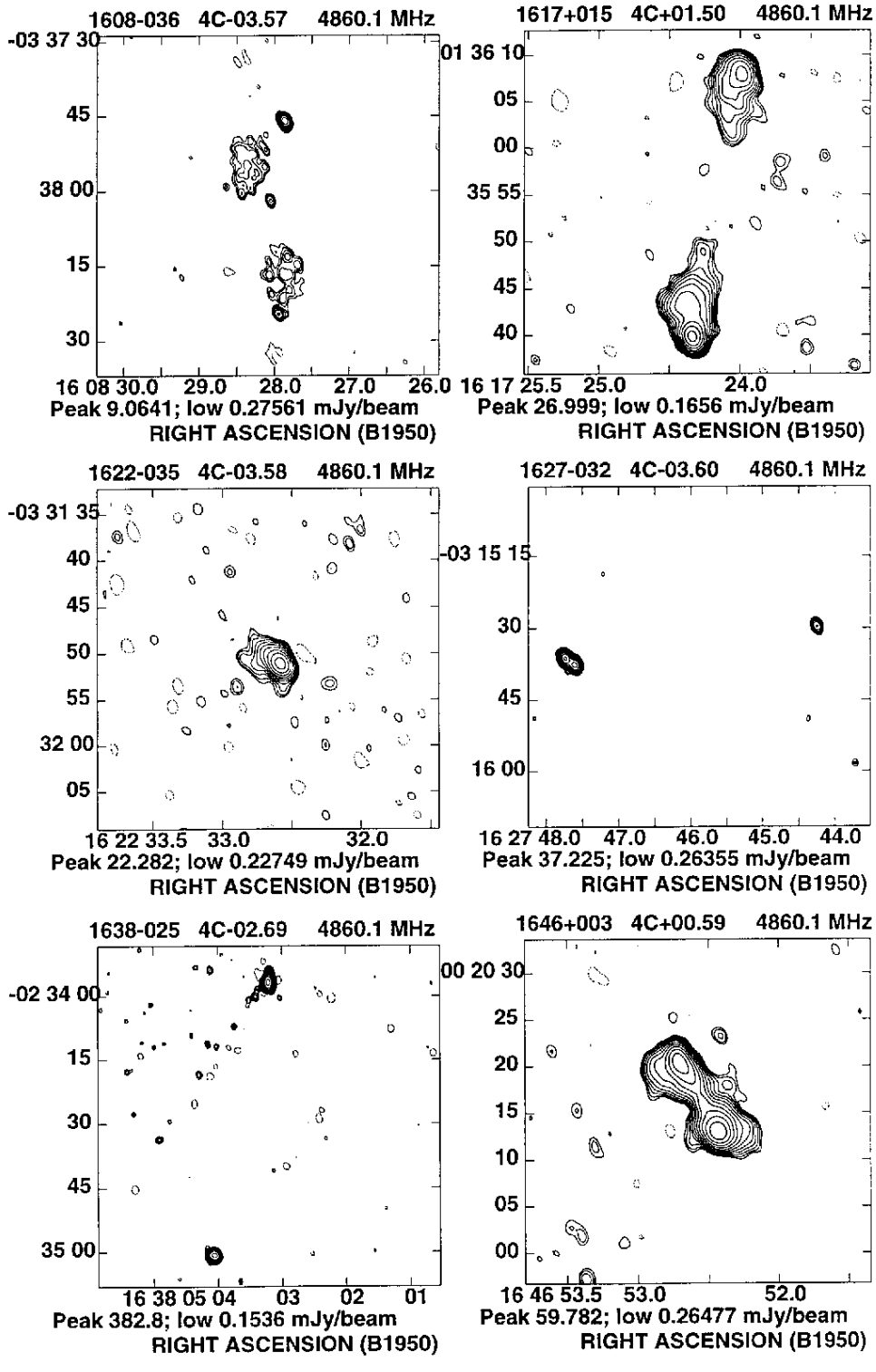

Fig. 1. continued

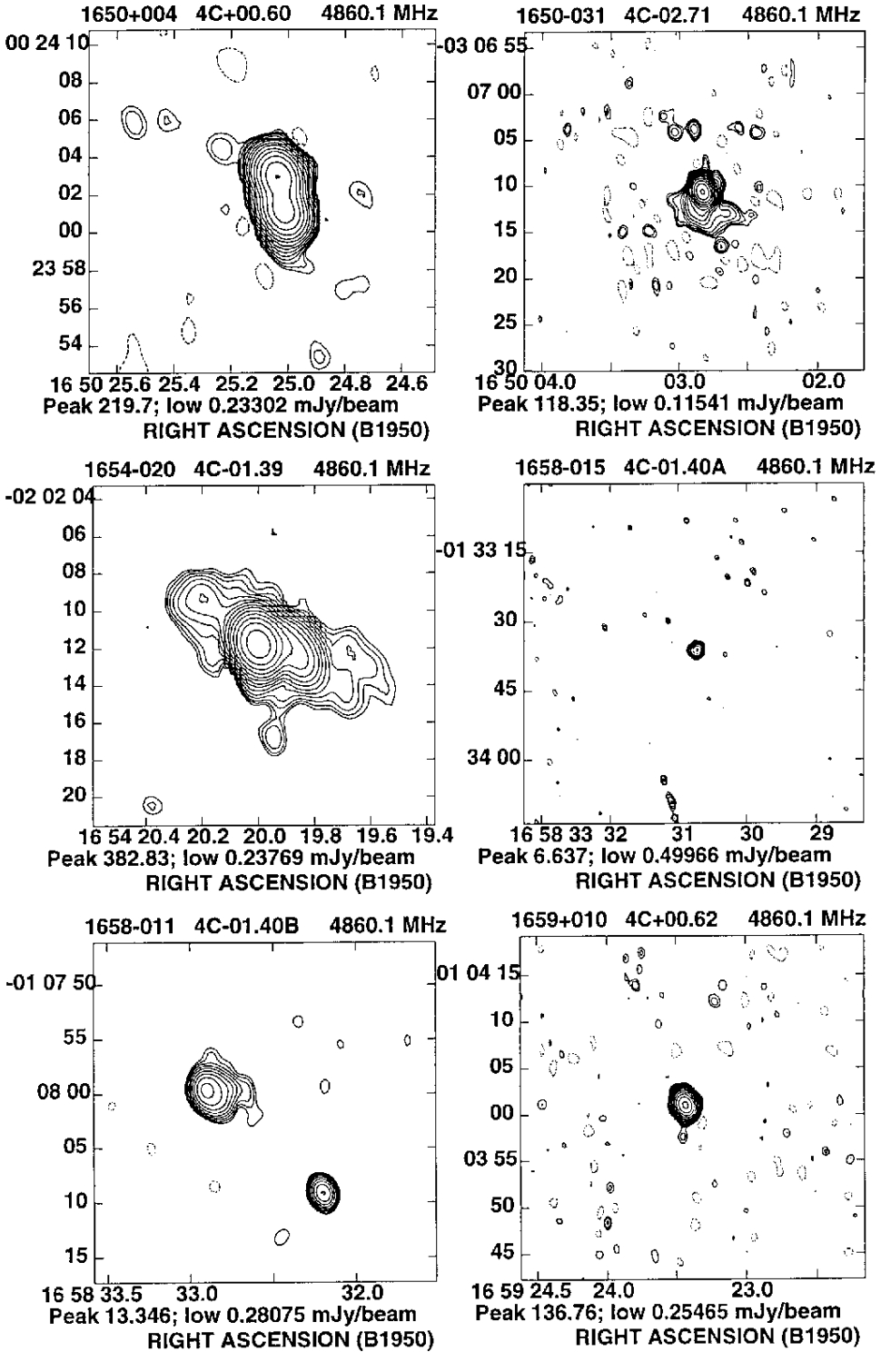

Fig. 1. continued

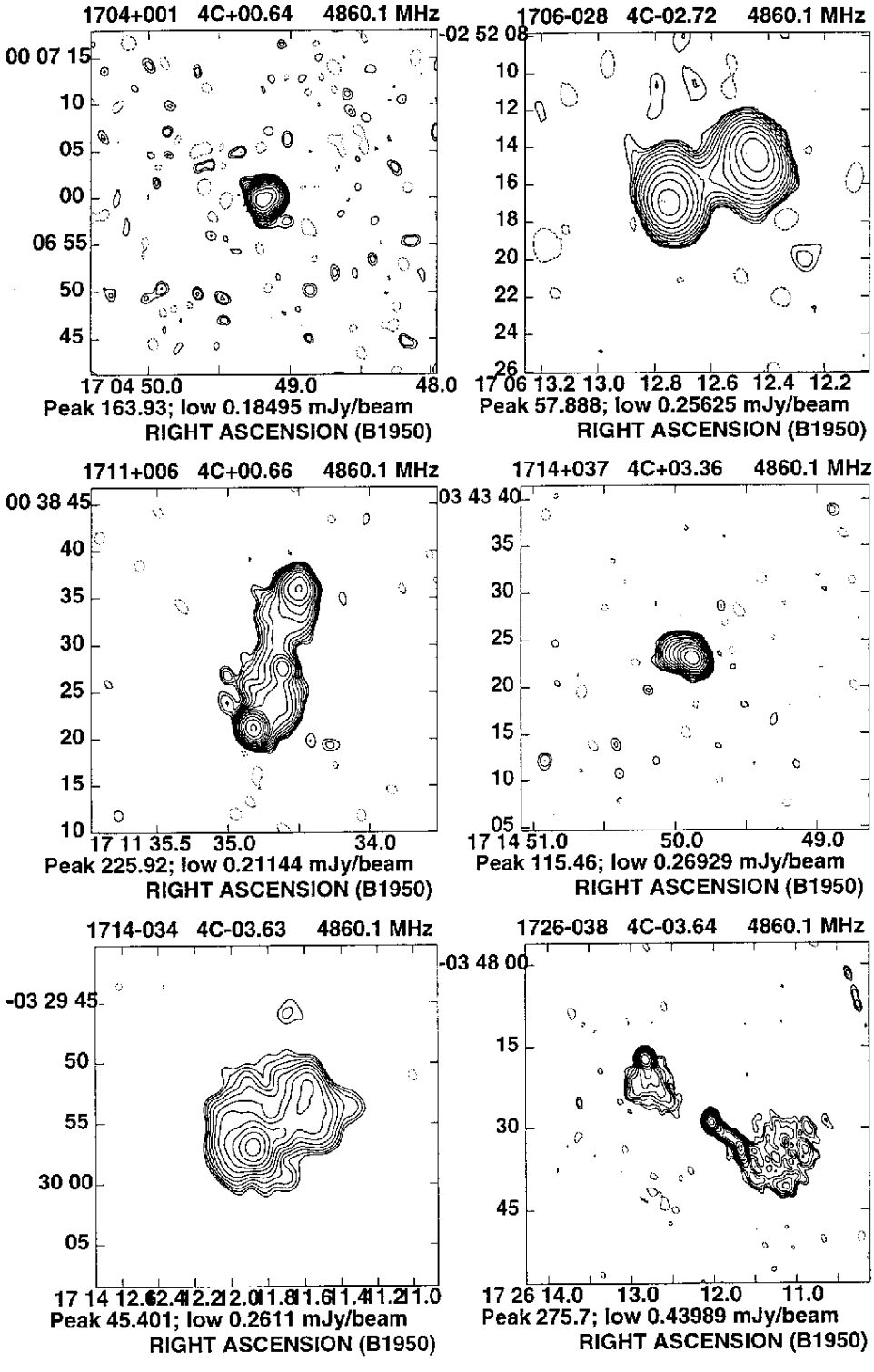

Fig. 1. continued

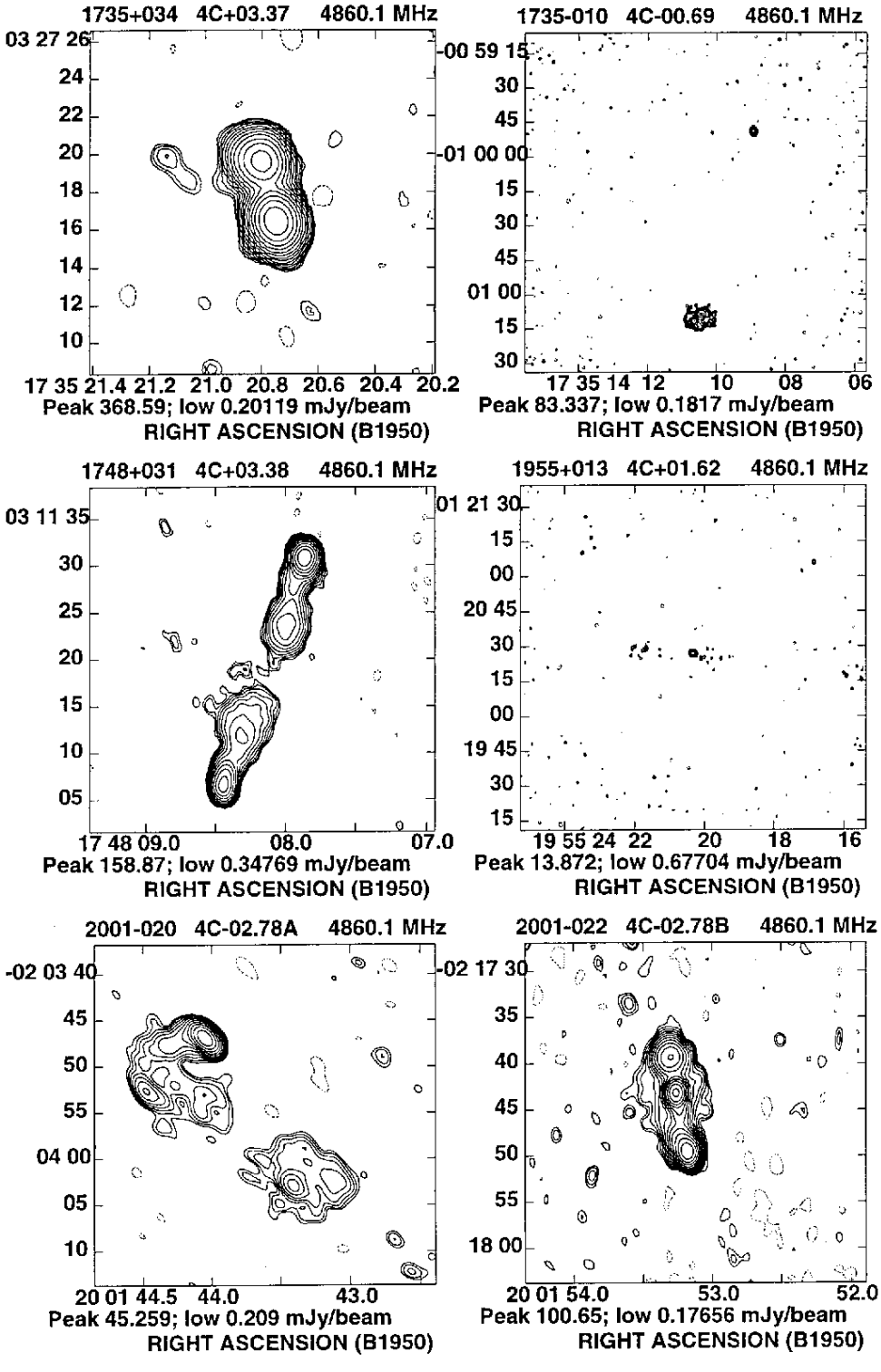

Fig. 1. continued

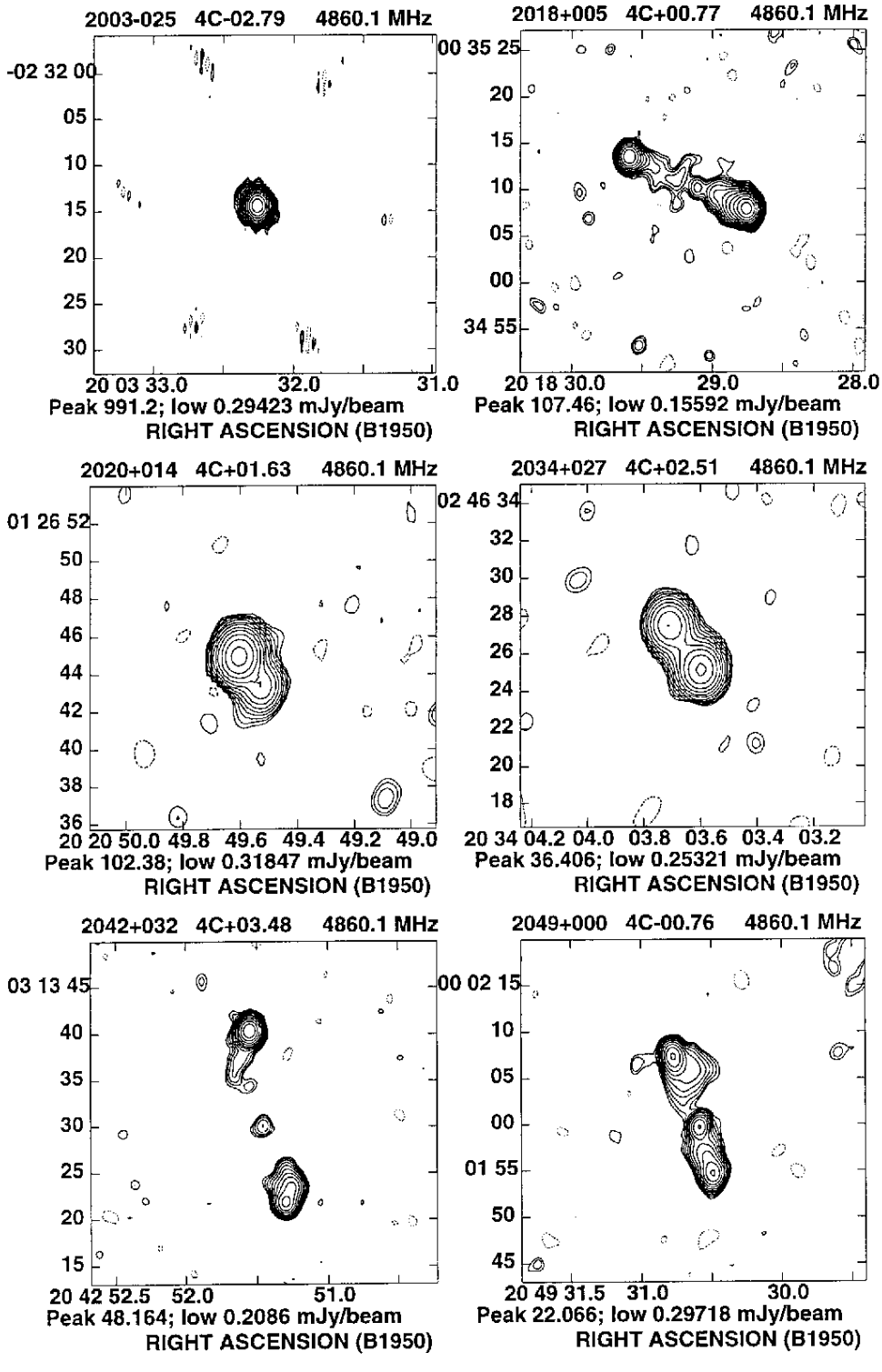

Fig. 1. continued

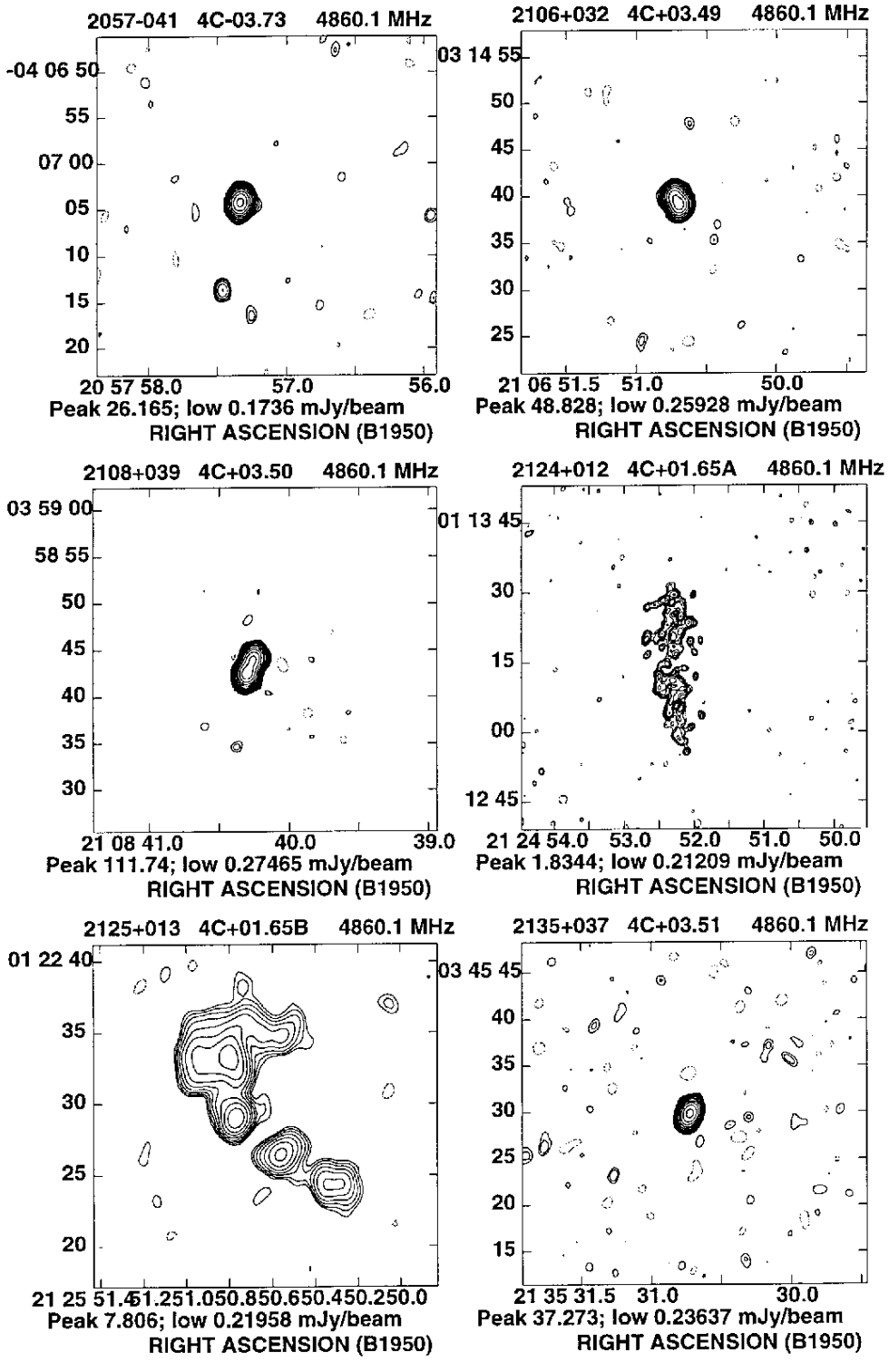

Fig. 1. continued

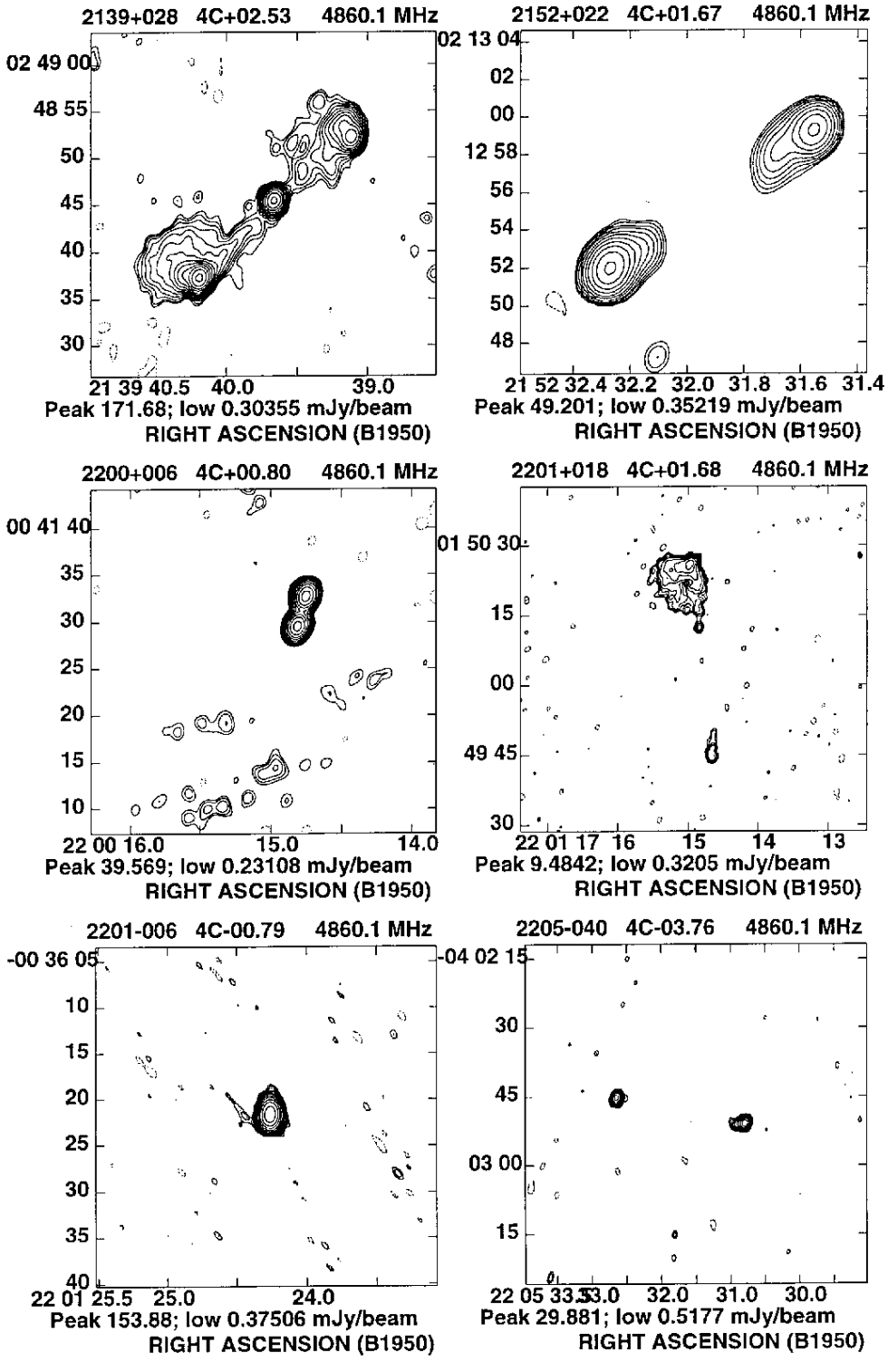

Fig. 1. continued

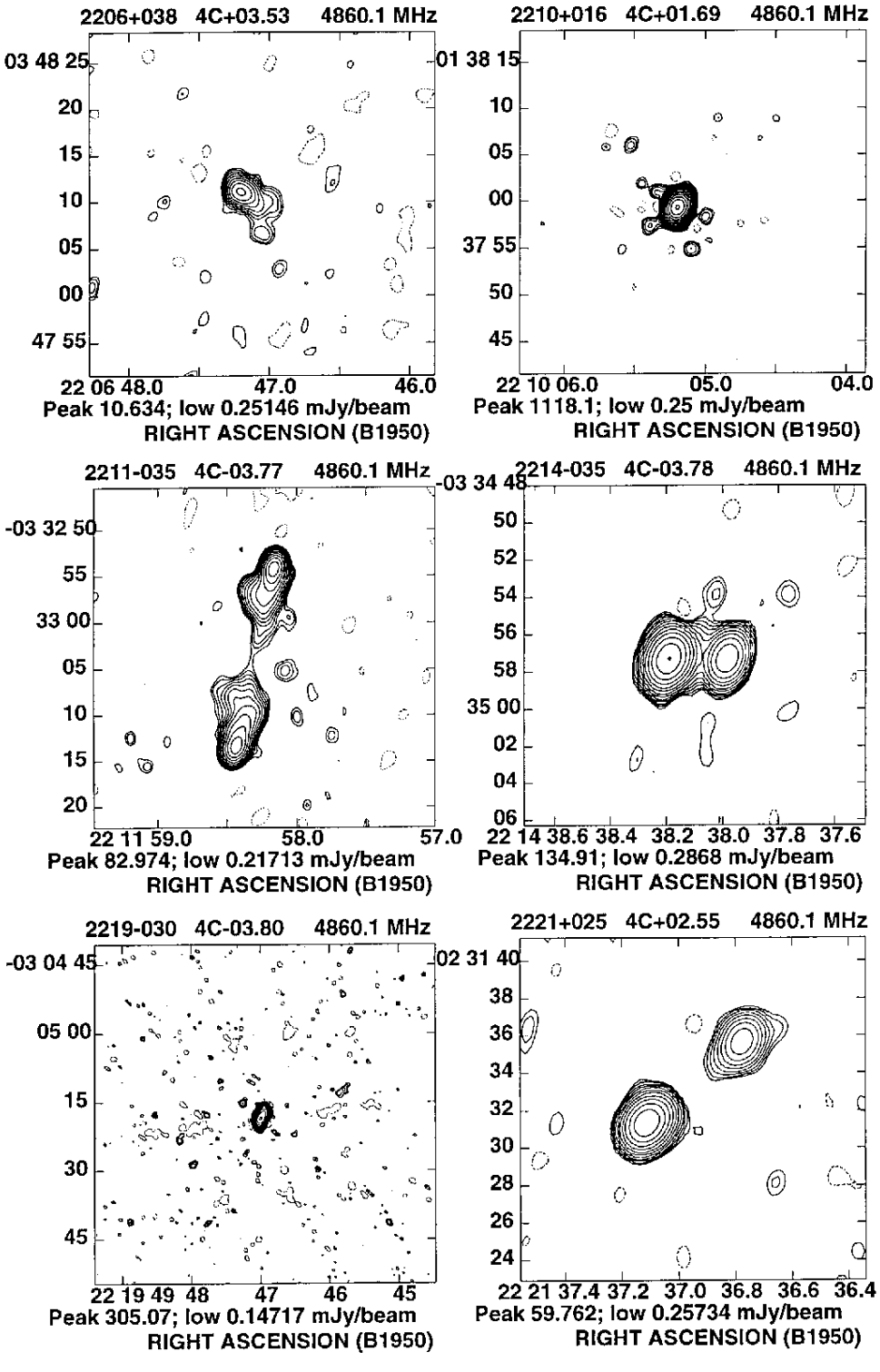

Fig. 1. continued

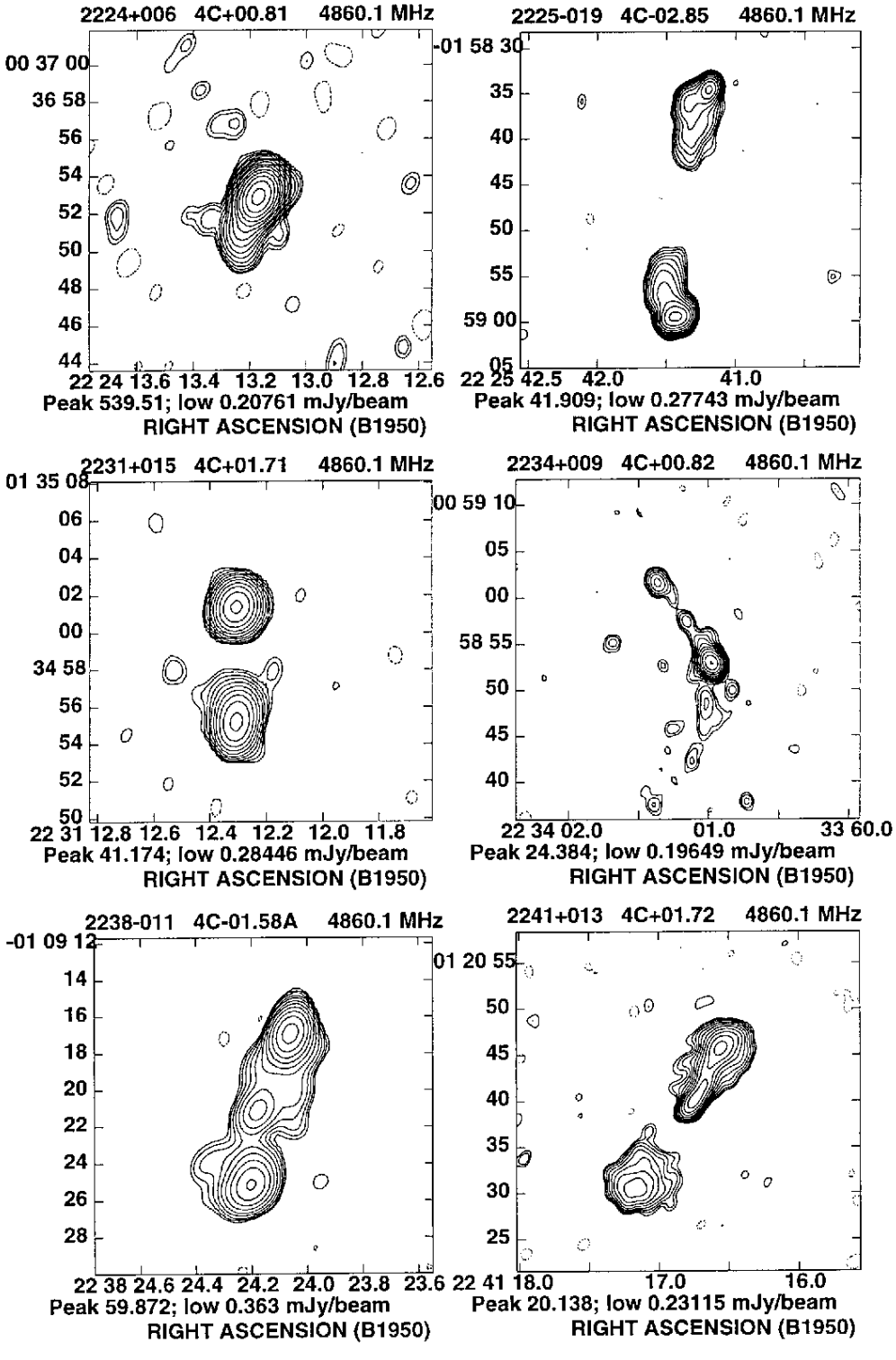

Fig. 1. continued

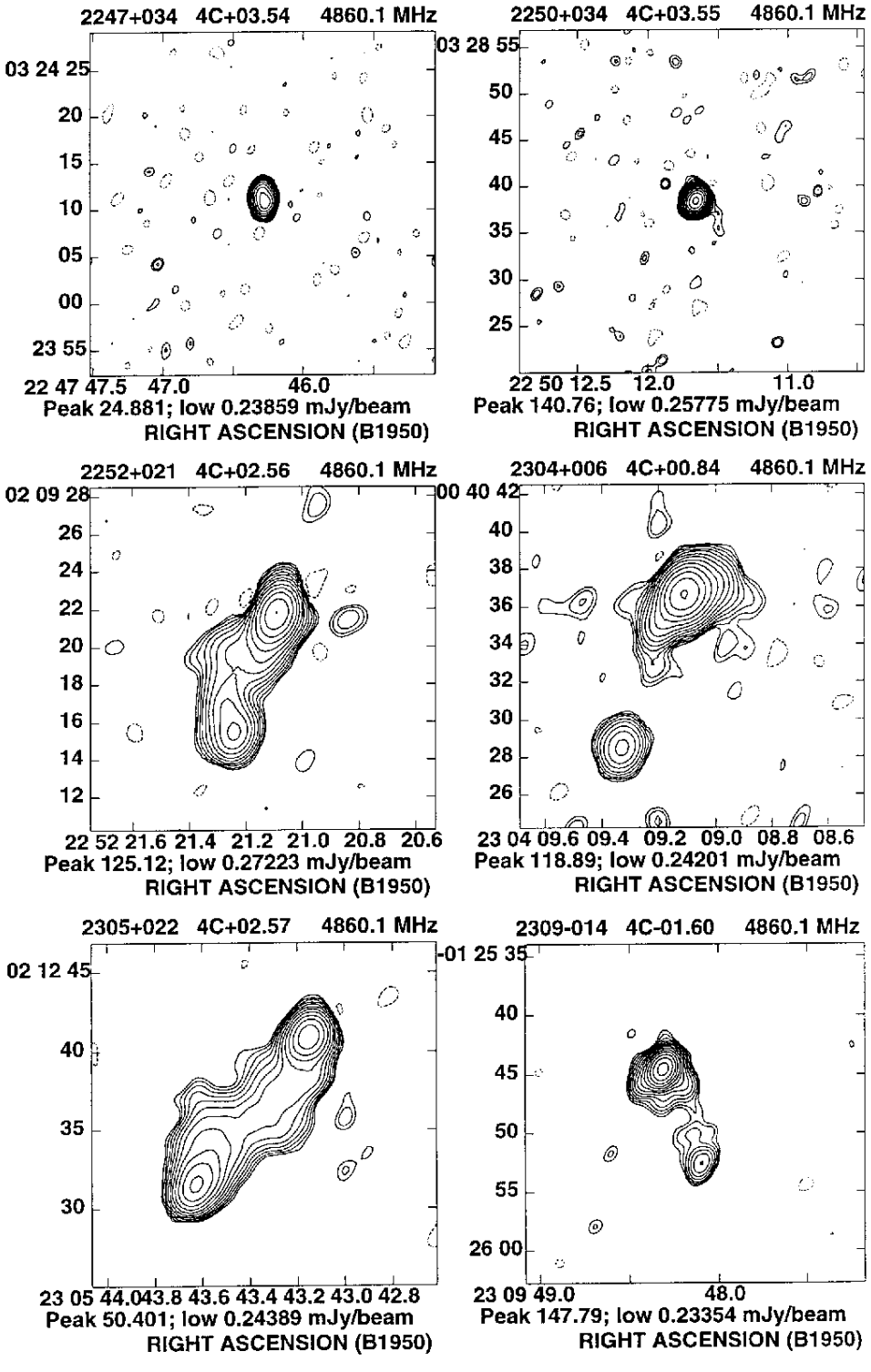

Fig. 1. continued

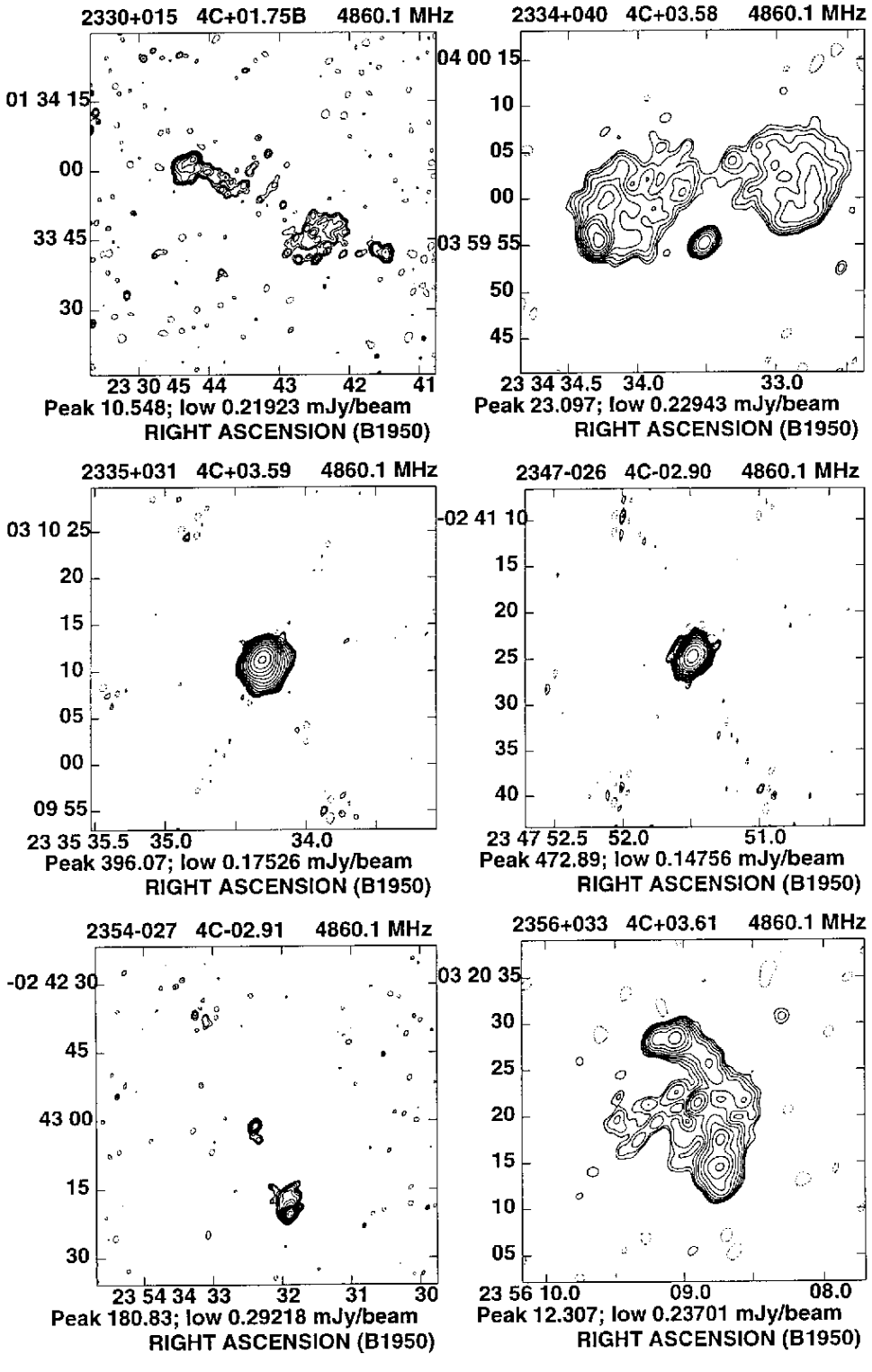

Fig. 1. continued

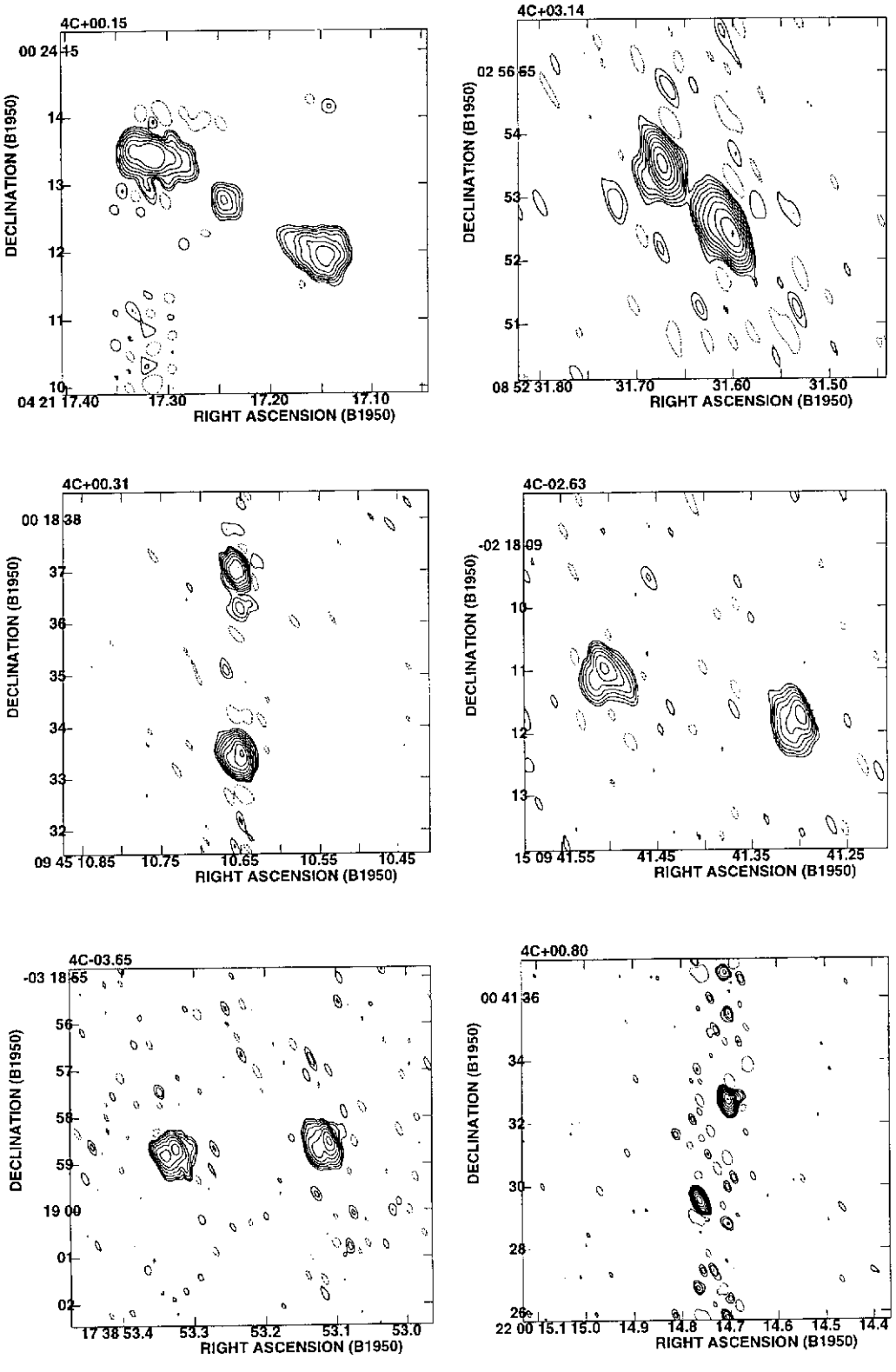

Fig. 2. MERLIN maps of six small sources observed in Paper I. Contours are given at $f\times$ (−1, 1, 2, 4, 8, 16, 32...) where f = 1 mJy/beam (4C+00.15), 0.5 mJy/beam (4C+03.14), 0.7 mJy/beam (4C+00.31), 0.5 mJy/beam (4C−02.63), 0.3 mJy/beam (4C−03.65), 1.5 mJy/beam (4C+00.80)